

Reconstructing Classes of Non-bandlimited Signals from Time Encoded Information

Roxana Alexandru, *Student Member*, IEEE, and Pier Luigi Dragotti, *Fellow*, IEEE

Abstract—We investigate time encoding as an alternative method to classical sampling, and address the problem of reconstructing non-bandlimited signals from time-based samples. We consider a sampling mechanism based on first filtering the input, before obtaining the timing information using a time encoding machine. Within this framework, we show that sampling by timing is equivalent to a non-uniform sampling problem, where the reconstruction of the input depends on the characteristics of the filter and on its non-uniform shifts. The classes of filters we focus on are exponential and polynomial splines, and we show that their fundamental properties are locally preserved in the context of non-uniform sampling. Leveraging these properties, we then derive sufficient conditions and propose novel algorithms for perfect reconstruction of classes of non-bandlimited signals. Next, we extend these methods to operate with arbitrary sampling kernels, and also present simulation results on synthetic noisy data.

Index Terms—Analog-to-digital conversion, non-uniform sampling, finite rate of innovation, time encoding machine, integrate-and-fire, crossing detector, splines.

I. INTRODUCTION

Sampling plays a fundamental role in signal processing and communications, achieving the conversion of continuous time phenomena into discrete sequences [1]. From the Whittaker-Shannon theorem [2], to recent theories in compressed sensing [3], [4], super-resolution [5] and finite rate of innovation [6]–[10], sampling theory has provided precise answers on when a faithful conversion of a continuous waveform into a discrete sequence is possible. These methods are generally based on recording the signal amplitude at specified times, which lead to uniform sampling if the samples are evenly spaced, and non-uniform sampling otherwise.

In this paper, we concentrate on an alternative method to classical sampling, which encodes the input into a sequence of non-uniformly spaced time events or *spikes*. In other words, rather than recording the value of the signal at preset times, one records the instants when the signal crosses a pre-defined threshold or triggers a pre-defined event.

Acquisition models inspired by this mechanism include zero crossing detectors [13], delta-modulation schemes [14], as well as the time encoding machine (TEM) introduced in [15]. This latter acquisition model is of particular interest, as it mimics the *integrate-and-fire* mechanism of neurons in the human brain. Biological neurons use time encoding to represent sensory information as a sequence of action potentials [16]–[18], which allows them to process information very efficiently. In the same manner, sampling inspired by the brain could lead to

very simple and highly efficient devices, ranging from analog to digital converters [15], to neuromorphic computing or event-based vision sensors, which record only changes in the input intensity, leading to low power consumption and fewer storage requirements [19]. Beyond that, the study of time encoding and decoding may bring us closer to understanding the neural language, which is one of the most important open problems in computational neuroscience.

At the same time, time-encoding methods extend theories of traditional sampling, and this makes this topic intriguing also from a research perspective. Within the study of time encoding, the key problem that arises is to find methods to retrieve the input signal from its timing information, and hence the key questions to pursue are the following. 1) Is time encoding invertible, and which classes of signals can be uniquely represented using timing information? 2) What algorithms allow perfect retrieval of these signals from their time-encoded samples?

To address these questions, several authors have provided ways to sample and reconstruct bandlimited signals [20]–[26], typically connecting time-based sampling with the problem of non-uniform sampling in shift-invariant spaces [27]–[30]. The fundamental limit of most of these methods is the underlying assumption that the input signal is bandlimited, and that its bandwidth is known. In reality, signals typically have finite time support, and therefore this assumption does not hold. Time encoding theory has been extended to the case of non-bandlimited signals in [31], however in the context of studying the dynamics of populations of neurons, by leveraging stochastic assumptions on the firing parameters.

In this paper, we focus on particular classes of continuous-time non-bandlimited signals such as streams and bursts of Diracs, streams of pulses as well as piecewise constant signals, and show that it is possible to perfectly reconstruct them from samples obtained using a time encoding mechanism. The time encoding strategy we propose is based on filtering the input signal, before extracting the timing information using a crossing or an integrate-and-fire TEM. We focus on two classes of filters (sampling kernels), exponential and polynomial splines. Our first main contribution is to prove that exponential (polynomial) splines locally preserve their exponential (polynomial) reproducing properties in the context of time-based sampling. Specifically, we show that within intervals where there are no knots of at least N non-uniformly shifted kernels, we can locally reproduce exponentials (polynomials) of degree N . The second aspect of our contribution is to leverage these properties to address the problem of reconstructing non-bandlimited signals from timing information. For the case of one Dirac, we show how a linear combination of its non-uniform samples leads to a sequence of signal moments, which can then be

Some of the work in this paper will, in part, be presented at the IEEE International Conference on Acoustics, Speech and Signal Processing (ICASSP), Brighton, United Kingdom, May 2019 [11], and the International Conference on Sampling Theory and Applications (SampTA), Bordeaux, France, July 2019 [12].

annihilated using Prony's method [32], in order to retrieve the free parameters of the input. Furthermore, we extend this method to reconstruct streams and bursts of Diracs, as well as piecewise constant signals. Finally, we depart from the ideal case, and present a universal reconstruction strategy that works with timing-based samples taken by arbitrary kernels.

This paper is organized as follows. In Section II-A, we describe the principles of time encoding, with two exemplary cases. Then, in Section II-B we show that sampling kernels which reproduce exponentials or polynomials preserve this property locally, when sampling is based on timing information. Furthermore, in Section III we present methods for reconstruction of non-bandlimited signals from their timing information obtained using a crossing TEM. We first propose a method for estimation of a single Dirac, and extend this to retrieval of streams of Diracs and bursts of Diracs. Then, in Section IV we demonstrate the perfect retrieval of classes of non-bandlimited signals from timing information, obtained using an integrate-and-fire TEM. These estimation methods are then extended in Section V to the case of arbitrary sampling kernels. Here we also present results for the case of noisy signals. Finally, we highlight the high efficiency of sampling based on timing information in Section VI, and present concluding remarks in Section VII.

II. TIME ENCODING MECHANISMS

A. Acquisition Models

In this section, we introduce the time encoding machines considered in this paper: the crossing TEM and the integrate-and-fire TEM. Specifically, we show how these TEMs map a real signal $x(t)$ to a strictly increasing sequence of times $\{t_n\}$ [30]. We also show that although no measure of the amplitude of the signal is recorded, time encoding is equivalent to a non-uniform sampling problem.

1) *Crossing Time Encoding Machine*: The crossing time encoding strategy is depicted in Fig. 1. It consists of a compact-support filter $\varphi(-t)$, and a comparator with a sinusoidal reference $g(t)$. The output of the acquisition device is the sequence $\{t_n\}$, corresponding to the time instants when the filtered input signal crosses the reference, i.e. when $y(t_n) - g(t_n) = 0$. Moreover, since the shape of the test function $g(t)$ is known, we can retrieve the amplitudes of the output samples, given by $y_n = y(t_n) = g(t_n)$. Hence, decoding the input signal is equivalent to a non-uniform sampling problem, where we aim to reconstruct $x(t)$ from the non-uniform samples given by:

$$y_n = y(t_n) = \int x(\tau)\varphi(\tau - t_n)d\tau = \langle x(t), \varphi(t - t_n) \rangle. \quad (1)$$

In Fig. 2 we depict the time encoded information of an input signal of 3 Diracs, obtained using the TEM in Fig. 1.

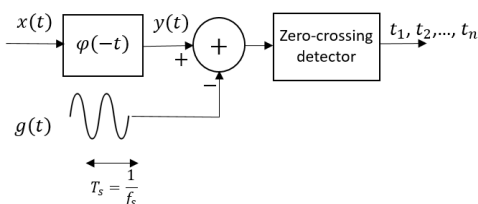


Fig. 1: Crossing Time Encoding Machine.

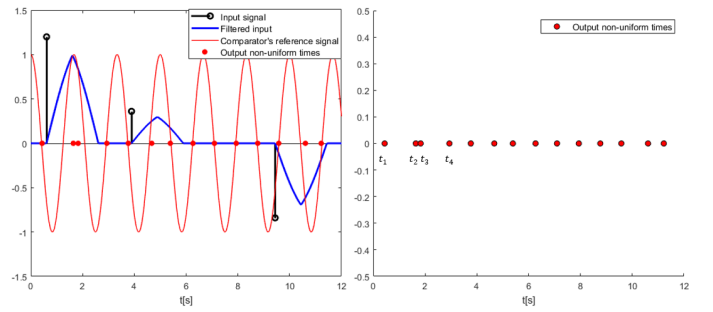


Fig. 2: Time encoding based on the Crossing TEM.

2) *Time Encoding based on an Integrate-and-fire System*: The operating principle of this time encoding strategy is similar to the one in [20], and is depicted in Fig. 3. The signal is first filtered with the compact-support filter $\varphi(-t)$, before being passed to an integrator. When the output of the integrator reaches the positive trigger mark C_T , the time encoding machine outputs a spike and the integrated signal $y(t)$ is reset to zero. Similarly, a spike is generated and $y(t)$ resets to zero, when the integrator reaches the negative trigger mark $-C_T$. The time instants when the integrator reaches the threshold $\pm C_T$ are recorded in the sequence $\{t_n\}$. Then, we can compute the output sample $y(t_n)$ at each spike t_n as:

$$y_n = y(t_n) = \pm C_T = \int_{t_{n-1}}^{t_n} f(\tau)d\tau, \quad (2)$$

where $n \geq 2$ and $f(t)$ is defined as:

$$f(t) = \int x(\alpha)\varphi(\alpha - t)d\alpha, \text{ for } t \in [t_{n-1}, t_n]. \quad (3)$$

Similarly, assuming that the input signal $x(t) = 0$, for $t < \tau_1$, and that the filter $\varphi(-t)$ is causal, then the first output sample is given by:

$$y_1 = y(t_1) = \pm C_T = \int_{\tau_1}^{t_1} f(\tau)d\tau. \quad (4)$$

Hence, time encoding with an integrate-and-fire model is equivalent to a non-uniform sampling problem, where we aim to estimate the input $x(t)$ from the non-uniform samples $y(t_n)$. In Fig. 4 we depict the time encoding of an input signal, obtained using the device in Fig. 3, for $C_T = 0.15$.

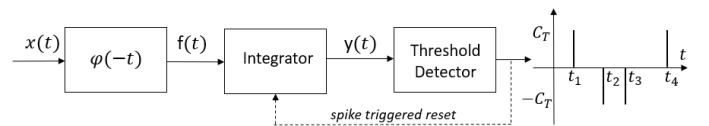


Fig. 3: Time Encoding Machine based on Integrate-and-fire.

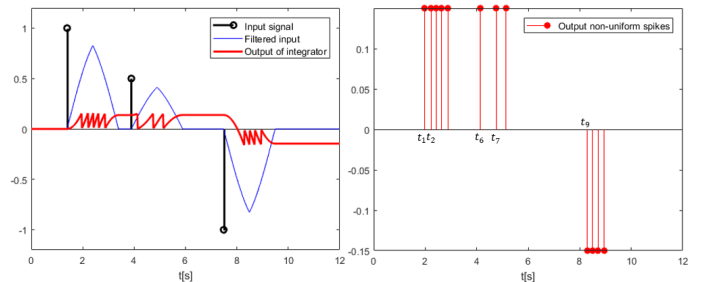


Fig. 4: Time Encoding based on the Integrate-and-fire TEM.

Furthermore, we can show that the non-uniform output samples we obtain using the acquisition model in Fig. 3 are the

same as those obtained by filtering the input with the modified kernel $(\varphi * q_{\theta_n})(t)$:

$$y(t_n) = \langle x(t), (\varphi * q_{\theta_n})(t - t_{n-1}) \rangle, \quad (5)$$

where $\theta_n = t_n - t_{n-1}$ and $q_{\theta_n}(t)$ is defined as:

$$q_{\theta_n}(t) = \begin{cases} 1, & 0 \leq t \leq \theta_n, \\ 0, & \text{otherwise.} \end{cases} \quad (6)$$

We can prove Eq. (5) by re-writing Eq. (2) as follows:

$$\begin{aligned} y(t_n) &= \int_{t_{n-1}}^{t_n} f(\tau) d\tau = \int_{t_{n-1}}^{t_n} \int_{-\infty}^{\infty} x(t) \varphi(t - \tau) dt d\tau \\ &\stackrel{(a)}{=} \int_{-\infty}^{\infty} x(t) \int_{t_{n-1}}^{t_n} \varphi(t - \tau) d\tau dt \\ &\stackrel{(b)}{=} \int_{-\infty}^{\infty} x(t) \int_{t-t_n}^{t-t_{n-1}} \varphi(\tau) d\tau dt \\ &\stackrel{(c)}{=} \int_{-\infty}^{\infty} x(t) \int_{t-t_n}^{t-t_{n-1}} \varphi(\tau) q_{\theta_n}(t - t_{n-1} - \tau) d\tau dt \\ &\stackrel{(d)}{=} \int_{-\infty}^{\infty} x(t) (\varphi * q_{\theta_n})(t - t_{n-1}) dt \\ &= \langle x(t), (\varphi * q_{\theta_n})(t - t_{n-1}) \rangle. \end{aligned} \quad (7)$$

In the derivations above, (a) holds since we assume both the input $x(t)$ and the filter $\varphi(t)$ have compact support, and (b) follows from a change of variable. Moreover, (c) follows from the fact that $q_{\theta_n}(t - t_{n-1} - \tau) = 1$ for $\tau \in [t - t_n, t - t_{n-1}]$ and (d) holds since $q_{\theta_n}(t - t_{n-1} - \tau) = 0$ for $\tau \notin [t - t_n, t - t_{n-1}]$, as defined in Eq. (6).

Finally, the first output sample can be computed as:

$$y(t_1) \stackrel{(a)}{=} \int_{\tau_1}^{t_1} f(\tau) d\tau = \langle x(t), (\varphi * q_{\theta_1})(t - \tau_1) \rangle, \quad (8)$$

where $\theta_1 = t_1 - \tau_1$, and (a) follows from Eq. (4).

We conclude this subsection by making the following remarks. First of all, we note that the proposed TEMs differ from those used in previous papers (e.g. [20]), since we assume that the signal $x(t)$ is filtered before being time encoded. The filter models the distortion introduced by the acquisition device and we denote with $\varphi(t)$ the time reversed version of its impulse response. We call $\varphi(t)$ the sampling kernel.

We also observe that from the timing sequence $\{t_n\}$, we can either recover $y(t_n) = \langle x(t), \varphi(t - t_n) \rangle$ for the case of the crossing TEM or $y(t_n) = \langle x(t), (\varphi * q_{\theta_n})(t - t_{n-1}) \rangle$ for the integrate-and-fire model. This means that in both cases, the reconstruction of $x(t)$ will depend on the proper choice of the sampling kernel $\varphi(t)$ and on its non-uniform shifts $\varphi(t - t_n)$.

In what follows we focus on two families of kernels, polynomial and exponential splines [6], [33], [34], and show that some of their fundamental properties are preserved in the case of non-uniform shifts.

B. Sampling Kernels

The sampling kernels $\varphi(t)$, that we consider in this paper are all anti-causal since they are the time reversed versions of causal filters.

1) *Polynomial splines*: A B-spline $\beta_P(t)$ of order P is computed as the $(P + 1)$ -fold convolution of the box function $\beta_0(t)$ [33]:

$$\beta_P(t) = \underbrace{\beta_0(t) * \beta_0(t) \dots * \beta_0(t)}_{P+1 \text{ times}}$$

where the anti-causal version of $\beta_0(t)$ is defined as:

$$\beta_0(t) = \begin{cases} 1, & -1 \leq t \leq 0, \\ 0, & \text{otherwise.} \end{cases}$$

The B-spline of order P satisfies the Strang-Fix conditions [35] and hence, together with its uniform shifts, it can reproduce polynomials of maximum degree P :

$$\sum_{n \in \mathbb{Z}} c_{m,n} \beta_P(t - n) = t^m, \quad (9)$$

where $m \in \{0, 1, \dots, P\}$, and for a proper choice of the coefficients $c_{m,n}$.

For instance, the first-order B-spline satisfies Eq. (9) for $P = 1$, which means it can reproduce constant and linear polynomials, and is defined as:

$$\beta_1(t) = \begin{cases} -t, & -1 \leq t \leq 0, \\ 2 + t, & -2 \leq t \leq -1, \\ 0, & \text{otherwise.} \end{cases}$$

The first order B-spline has two continuous regions, each of which is a linear polynomial: $\beta_1^A(t) = -t$, for $t \in [-1, 0]$ and $\beta_1^B(t) = 2 + t$, for $t \in [-2, -1]$. Using this observation, it is possible to show that the first-order B-spline, together with its *non-uniformly* shifted versions can *locally* reproduce polynomials of maximum degree 1. In other words, it is possible to prove that within a time interval I where the shifted kernels $\beta_1(t - t_n)$ have no discontinuities, the following equations holds:

$$\sum_{n=0}^{N-1} c_{m,n}^I \beta_1(t - t_n) = t^m, \quad (10)$$

where $N \geq 2$, $m \in \{0, 1\}$, $t \in I$ and $\{t_n\}$ are non-uniform.

The proof can be outlined by setting $N = 2$ for simplicity. Then, let I be an interval where there are no knots of $\beta_1(t - t_0)$ and $\beta_1(t - t_1)$, with $I \subset [t_1 - 2, t_0 - 1]$. Furthermore, let $v_0(t) = \beta_1(t - t_0) = -t + t_0$ for $t \in I$ and $v_1(t) = \beta_1(t - t_1) = -t + t_1$ for $t \in I$. In the vector space of linear polynomials in I , the elements $v_0(t)$ and $v_1(t)$ are linearly independent, provided $t_0 \neq t_1$. Therefore, using a linear combination of the two functions, we can uniquely represent any vector in this space, including the vector t . In other words, we can determine the unique coefficients $c_{1,0}^I = \frac{t_1}{t_0 - t_1}$ and $c_{1,1}^I = \frac{t_0}{t_1 - t_0}$ that ensure $c_{1,0}^I v_0(t) + c_{1,1}^I v_1(t) = t$, for $t \in I$. Similarly, we find the unique coefficients $c_{0,0}^I = \frac{1}{t_0 - t_1}$ and $c_{0,1}^I = \frac{1}{t_1 - t_0}$ such that $c_{0,0}^I v_0(t) + c_{0,1}^I v_1(t) = 1$, for $t \in I$. Hence, Eq. (10) is satisfied in the knot-free interval I for $N = 2$.

In the same manner, one can show that reproduction of constant and linear polynomials is achieved on any interval spanned by knot-free regions of at least two non-uniformly shifted B-splines. Lastly but importantly, for different knot-free intervals, the solution to Eq. (10) differs, and this fact is highlighted in Fig. 5. Here, we depict two non-uniform shifts of the first-order B-spline, namely $\beta_1(t - 2)$ and $\beta_1(t - 2.625)$. The shifted kernel $\beta_1(t - 2)$ has knots at $t = 0$, $t = 1$ and $t = 2$, whilst $\beta_1(t - 2.625)$ has knots at $t = 0.625$, $t = 1.625$ and $t = 2.625$. As a result, reproduction of polynomials is possible within the knot-free regions $I_1 = [0.625, 1]$ and $I_2 = [1, 1.625]$, however with a different linear combination of the B-splines overlapping these regions, i.e. with $c_{m,n}^{I_1} \neq c_{m,n}^{I_2}$.

One can extend this result to the case of higher order polynomials by using B-splines of order $P > 1$. This is due

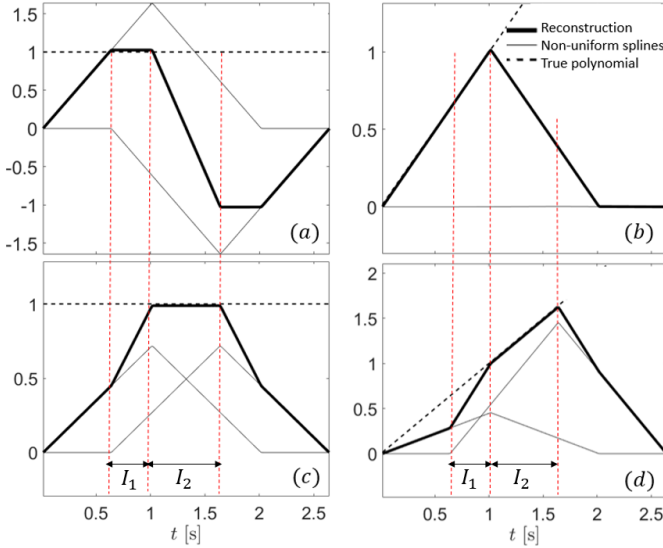


Fig. 5: Reproduction of constant and linear polynomials in two different time intervals, $I_1 = [0.625, 1]s$ in (a) and (b), and $I_2 = [1, 1.625]s$ in (c) and (d). In this case, two knot-free regions of two non-uniformly shifted first-order B-splines overlap I_1 and I_2 .

to the fact that polynomial splines are piecewise polynomial functions of degree P . Hence, in any interval I that contains $P + 1$ knot-free shifted versions of splines, it is possible to reproduce polynomials up to degree P .

2) *Exponential splines*: The anti-causal version of the E-spline of first-order is defined as:

$$\varphi_1(t) = \begin{cases} e^{-\alpha_0 t}, & -1 \leq t \leq 0, \\ 0, & \text{otherwise.} \end{cases}$$

where α_0 can be either real or complex.

As with polynomial splines, E-splines of order P are obtained from the convolution of first-order E-splines [34]:

$$\varphi_P(t) = \varphi_{\alpha_0}(t) * \varphi_{\alpha_1}(t) \dots * \varphi_{\alpha_{P-1}}(t). \quad (11)$$

An E-spline of order P has compact support and can reproduce P different exponentials of the form $e^{-\alpha_m t}$ [34]:

$$\sum_{n \in \mathbb{Z}} c_{m,n} \varphi(t-n) = e^{-\alpha_m t},$$

where $m = 0, 1, \dots, P$, and for a suitable choice of the coefficients $c_{m,n}$.

For example, the E-spline of order $P = 2$ of support L is defined as:

$$\varphi_2(t) = \begin{cases} \frac{e^{\alpha_1 - \alpha_0}}{\alpha_1 - \alpha_0} e^{-\alpha_0 t} + \frac{e^{-\alpha_1 + \alpha_0}}{\alpha_0 - \alpha_1} e^{-\alpha_1 t}, & -L \leq t \leq -\frac{L}{2}, \\ \frac{1}{\alpha_0 - \alpha_1} e^{-\alpha_0 t} + \frac{1}{\alpha_1 - \alpha_0} e^{-\alpha_1 t}, & -\frac{L}{2} \leq t \leq 0, \\ 0, & \text{otherwise} \end{cases} \quad (12)$$

The second-order E-spline can reproduce the exponentials $e^{-\alpha_0 t}$ and $e^{-\alpha_1 t}$. In fact, we notice that within each of its knot-free regions, the function $\varphi_2(t)$ can be expressed as a linear combination of the exponentials $e^{-\alpha_0 t}$ and $e^{-\alpha_1 t}$. This observation helps us prove that within any time interval I which contains knot-free regions of non-uniformly shifted first-order E-splines, we can reproduce two exponentials:

$$\sum_{n=0}^{N-1} c_{m,n}^I \varphi_2(t-t_n) = e^{-\alpha_m t}, \quad (13)$$

where $N \geq 2$, $m \in \{0, 1\}$, $t \in I$ and $\{t_n\}$ are non-uniform.

For example, let I be an interval which contains knot-free regions of $\varphi_2(t-t_0)$ and $\varphi_2(t-t_1)$, with $I \subset [t_1 - L, t_0 - \frac{L}{2}]$.

Moreover, let $v_0(t) = \varphi_2(t-t_0)$ for $t \in I$ and $v_1(t) = \varphi_2(t-t_1)$ for $t \in I$. The elements $v_0(t)$ and $v_1(t)$ are linear combinations of $e^{-\alpha_0 t}$ and $e^{-\alpha_1 t}$, and therefore belong to the vector space spanned by these two exponentials. Moreover, $v_0(t)$ and $v_1(t)$ are linearly independent in that vector space, since $t_1 \neq t_0$. Hence, using a linear combination of v_0 and v_1 , we can uniquely represent any vector in this space, including $e^{-\alpha_0 t}$ and $e^{-\alpha_1 t}$. Therefore, in the interval I where there are no knots, we can find unique coefficients $c_{m,0}^I$ and $c_{m,1}^I$ such that Eq. (13) holds for $m \in \{0, 1\}$.

Similarly, reproduction of two different exponentials is possible on any time interval spanned by knot-free regions of at least two shifted E-splines. Note that for different intervals I_1 and I_2 , the solution to Eq. (13) differs, i.e. $c_{m,n}^{I_1} \neq c_{m,n}^{I_2}$. This is highlighted in Fig. 6, where exponential reproduction is possible in the regions I_1 and I_2 , but using a different linear combination of the E-splines that overlap these regions.

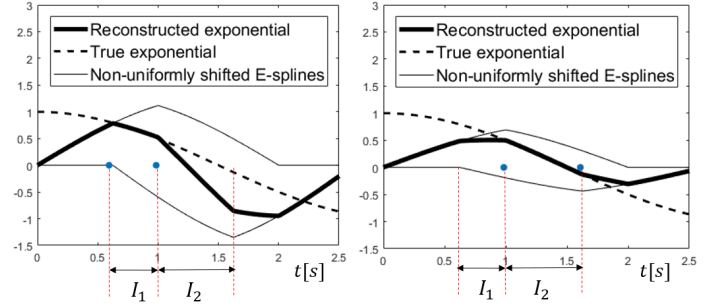


Fig. 6: Reproduction of $e^{j\frac{2\pi}{5}t}$ in two different intervals, $I_1 = [0.625, 1]s$ and $I_2 = [1, 1.625]s$, overlapped by continuous regions of two non-uniformly shifted second-order E-splines.

By using the same argument we can prove similar results for the general case of an E-spline of order P and support L which can reproduce P different exponentials. Specifically, within an interval I containing knot-free regions of at least P non-uniformly shifted E-splines, we can reproduce P different exponentials, such that Eq. (13) holds for $N \geq P$ and $m \in \{0, 1, \dots, P-1\}$. This is due to the fact that any knot-free interval of an E-spline of order P is a linear combination of P different exponentials.

Finally, let us consider the kernel $(\varphi_P * g)(t)$, where $\varphi_P(t)$ is a P -order E-spline which can reproduce the exponentials $e^{\alpha_m t}$, for $m = 0, 1, \dots, P-1$. Furthermore, let us assume that $g(t)$ has compact support and that its derivatives satisfy one of the following two conditions: $g^{(K-L)}(t) = cg^{(K)}(t)$ or $g^{(K)}(t) = 0$ for some $L, K \in \mathbb{N}$ with $K \geq L$ and constant $c \in \mathbb{C}$. Then, each continuous region $v(t)$ of $(\varphi_P * g)(t)$ can be expressed as a linear combination of $P + K$ independent elements, namely $v(t) = \sum_{m=0}^{P-1} a_m e^{\alpha_m t} + \sum_{k=0}^{K-1} b_k g^{(k)}(t)$, where $g^{(k)}(t)$ is the k^{th} derivative of $g(t)$. As a result, one can show that within an interval I spanned by knot-free regions of at least $P + K$ non-uniformly shifted kernels $(\varphi_P * g)(t-t_n)$, we can reproduce P different exponentials:

$$\sum_{n=0}^{P+K-1} c_{m,n}^I (\varphi_P * g)(t-t_n) = e^{\alpha_m t}, \quad (14)$$

where $m \in \{0, 1, \dots, P-1\}$, $t \in I$, and $\{t_n\}$ are non-uniform.

III. PERFECT RECOVERY OF SIGNALS FROM TIMING INFORMATION OBTAINED WITH A CROSSING TEM

In the previous section, we have mapped time encoding to non-uniform sampling. In what follows we assume that the sampling kernel $\varphi(t)$ is a second-order exponential reproducing spline, such that a linear combination of its non-uniformly shifted versions can reproduce two different exponentials, as described in Section II-B2. Moreover, $\varphi(t)$ has compact support L , with $\varphi(t) = 0$ for $t \notin [-L, 0]$ and the two frequencies that this kernel can reproduce are $\alpha_0 = j\omega_0$ and $\alpha_1 = -\alpha_0$, which ensures that $\varphi(t)$ is a real-valued function. Under these assumptions, we study the problem of reconstructing different classes of non-bandlimited signals, from timing information obtained using the crossing TEM in Fig. 1. Specifically we present a method for estimation of an input Dirac and extend this to retrieval of streams of Diracs and bursts of Diracs. We note that similar results could be proved using polynomial splines, but we omit these proofs to keep the focus of the paper on E-splines.

A. Estimation of an Input Dirac

Let us consider a single input Dirac of amplitude $|x_1| < 1$:

$$x(t) = x_1\delta(t - \tau_1). \quad (15)$$

Proposition 1. *The timing information t_1, t_2, \dots, t_M provided by the device in Fig. 1 is a sufficient representation of an input Dirac as in Eq. (15), when the reference signal $g(t) = A \cos(\omega_s t)$ has amplitude $A > 1$, and period $T_s \leq \frac{2L}{5}$, with L being the support of the sampling kernel $\varphi(t)$. Moreover, $\varphi(t)$ is a second-order E-spline that reproduces the exponentials $e^{j\omega_0 t}$ and $e^{j\omega_1 t}$, with $\omega_1 = -\omega_0$ and $0 < \omega_0 \leq \frac{\pi}{L}$.*

Proof. From the timing information t_1, t_2, \dots, t_M , we can retrieve the non-uniform output samples $y(t_1), y(t_2), \dots, y(t_M)$, as described in Eq. (1). Moreover, for simplicity, suppose that the amplitude of the input Dirac satisfies $x_1 > 0$. In addition, the hypothesis that $\varphi(t)$ reproduces $e^{\pm j\omega_0 t}$ with $0 < \omega_0 \leq \frac{\pi}{L}$ means that $0 \leq \varphi(t) < 1, \forall t$. Then, since $0 < x_1 < 1$, the output $y(t) = x_1\varphi(\tau_1 - t)$ of the crossing TEM satisfies $0 \leq y(t) < 1 < A = \max(g(t))$.

Let us define the continuous function $h(t) = g(t) - y(t)$. Using Bolzano's intermediate value theorem [36] and the fact that $0 \leq y(t) < \max(g(t))$, one can show that within the interval $[\tau_1, \tau_1 + \frac{5T_s}{4}]$, the function $h(t)$ crosses zero at least twice. In other words, $\exists t_1, t_2 \in [\tau_1, \tau_1 + \frac{5T_s}{4}]$ such that $h(t_1) = h(t_2) = 0$. For example, if we assume $h(\tau_1) = g(\tau_1) > 0$, then $g(\tau_1 + \frac{T_s}{2}) < 0$ and since $y(t) \geq 0 \forall t$, we get $h(\tau_1 + \frac{T_s}{2}) = g(\tau_1 + \frac{T_s}{2}) - y(\tau_1 + \frac{T_s}{2}) < 0$. Then, Bolzano's intermediate value theorem states that $\exists t_1 \in [\tau_1, \tau_1 + \frac{T_s}{2}]$ such that $h(t_1) = 0$. Using the same argument one can then show that $\exists t_2 \in [\tau_1 + \frac{T_s}{2}, \tau_1 + \frac{5T_s}{4}]$ such that $h(t_2) = 0$.

Hence, since we assume $\frac{L}{2} \geq \frac{5T_s}{4}$, we obtain the inequality $t_2 \leq \tau_1 + \frac{5T_s}{4} \leq \tau_1 + \frac{L}{2}$. This guarantees that in a region $[\tau_1, \tau_1 + \frac{L}{2}]$ following a Dirac at τ_1 , there are at least 2 output samples, namely $y(t_1)$ and $y(t_2)$, as depicted in Fig. 7.

Then, in the interval $I = [t_2 - \frac{L}{2}, t_1]$, which does not contain knots of either $\varphi(t - t_1)$ or $\varphi(t - t_2)$, we can reproduce two exponentials as described in Section II-B2. Specifically, we can find coefficients $c_{m,n}^I$ such that:

$$\sum_{n=1}^2 c_{m,n}^I \varphi(t - t_n) = e^{j\omega_m t}, \text{ for } m \in \{0, 1\}. \quad (16)$$

We then define the signal moments s_m as follows:

$$\begin{aligned} s_m &= \sum_{n=1}^2 c_{m,n}^I y(t_n) \stackrel{(a)}{=} \sum_{n=1}^2 c_{m,n}^I \langle x(t), \varphi(t - t_n) \rangle \\ &\stackrel{(b)}{=} \int_{-\infty}^{\infty} x(t) \sum_{n=1}^2 c_{m,n}^I \varphi(t - t_n) dt \\ &\stackrel{(c)}{=} \int_{-\infty}^{\infty} x_1 \delta(t - \tau_1) \sum_{n=1}^2 c_{m,n}^I \varphi(t - t_n) dt \\ &\stackrel{(d)}{=} \int_I x_1 \delta(t - \tau_1) e^{j\omega_m t} dt = x_1 e^{j\omega_m \tau_1} = b_1 u_1^m, \end{aligned} \quad (17)$$

where $b_1 := x_1 e^{j\omega_0 \tau_1}$, $u_1 := e^{j\lambda \tau_1}$, the frequencies $\omega_m = \omega_0 + \lambda m$, for $m \in \{0, 1\}$, and $\lambda = -2\omega_0$.

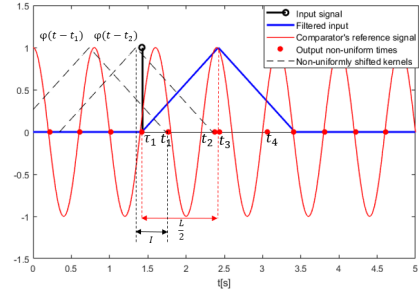


Fig. 7: Timing information obtained by encoding an input Dirac located at $\tau_1 \in I$, when $\frac{L}{2} > \frac{5T_s}{4}$.

The unknowns $\{b_1, u_1\}$ can be uniquely retrieved from the signal moments, using the annihilating filter method [37], also known as Prony's method [32] (see Appendix A). Then, we get the Dirac's amplitude and location, using $b_1 = x_1 e^{j\omega_0 \tau_1}$ and $u_1 = e^{j\lambda \tau_1}$.

In these derivations, (a) follows from Eq. (1), (b) from the linearity of the inner product, and (c) from Eq. (15). Moreover, (d) holds since $t_1, t_2 \in [\tau_1, \tau_1 + \frac{L}{2}]$, which means $\tau_1 \in I$, and from the local exponential reproduction property of $\varphi(t)$ in the region I , as given in Eq. (16).

Finally, one can prove that the derivations in Eq. (17) hold in any interval $I = [t_N - \frac{L}{2}, t_1]$ where there are no knots of any kernel $\varphi(t - t_n)$, for $t_n \in [\tau_1, \tau_1 + \frac{L}{2}]$, $n = 0, 1, \dots, N$ and $N \geq 2$. In this case, $s_m = \sum_{n=1}^N c_{m,n}^I y(t_n) = x_1 e^{j\omega_m \tau_1}$. \square

B. Estimation of a Stream of Diracs

Let us now consider the case of a stream of Diracs:

$$x(t) = \sum_k x_k \delta(t - \tau_k), \quad (18)$$

where $|x_k| < 1$.

Proposition 2. *The timing information t_1, t_2, \dots, t_M provided by the device shown in Fig. 1 is a sufficient representation of a stream of Diracs as in Eq. (18), when the reference signal $g(t) = A \cos(\omega_s t)$ has amplitude $A > 1$ and period $T_s \leq \frac{2L}{5}$, with L being the support of the sampling kernel $\varphi(t)$, and provided the minimum spacing between Diracs is larger than L . Moreover, the kernel $\varphi(t)$ is a second-order E-spline that reproduces the complex exponentials $e^{j\omega_0 t}$ and $e^{j\omega_1 t}$, with $\omega_1 = -\omega_0$ and $0 < \omega_0 \leq \frac{\pi}{L}$.*

Proof. Using the output samples $y(t_1)$ and $y(t_2)$, we can uniquely estimate the first Dirac in the stream using the method

in Section III-A. Furthermore let us denote with $y(t_n)$ and $y(t_{n+1})$ the first two samples located after $\tau_1 + L$. Since we assume that the separation between input Diracs is larger than the kernel's support L , then the location τ_2 of the second Dirac satisfies $\tau_1 + L < \tau_2 < t_n$. Moreover, provided the period of the comparator's signal satisfies $T_s \leq \frac{2L}{5}$, Bolzano's intermediate value theorem [36] guarantees that $y(t_n), y(t_{n+1}) \in [\tau_2, \tau_2 + \frac{L}{2}]$, as previously outlined in Section III-A. Then, the interval $I = [t_{n+1} - \frac{L}{2}, t_n]$ contains no knots of either $\varphi(t - t_n)$ or $\varphi(t - t_{n+1})$, and perfect exponential reproduction can be achieved. Hence we can compute the signal moments using similar derivations as in Eq. (17):

$$s_m = c_{m,n}^I y(t_n) + c_{m,n+1}^I y(t_{n+1}) = x_2 e^{j\omega_m \tau_2}.$$

Finally, we can estimate x_2 and τ_2 from s_m , using Prony's method. Once the second Dirac has been estimated, we use subsequent non-uniform output samples after $\tau_2 + L$ in order to sequentially retrieve the next Diracs. \square

The sampling and reconstruction of a stream of Diracs are depicted in Fig. 8. Here, the filter is a second-order E-spline, of support $L = 2$, which can reproduce the exponentials $e^{\pm j\frac{\pi}{3}t}$, and is shown in Fig. 8(b). Moreover, the frequency of the comparator's test signal is $f_s = 1.26 > \frac{5}{2L}$ and the separation between Diracs is at least L . The amplitudes and locations of the estimated Diracs are exact to numerical precision.

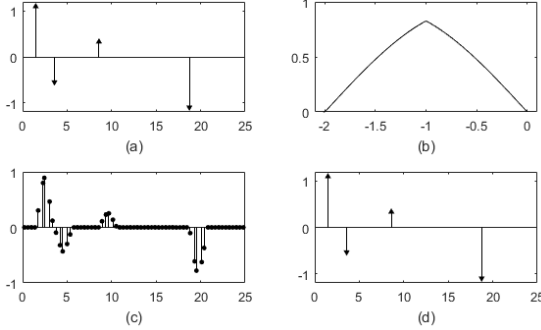


Fig. 8: Sampling of a stream of Diracs using the crossing TEM. The input signal is shown in (a), the sampling kernel in (b), the output non-uniform samples in (c), and the reconstructed signal in (d).

C. Multi-channel Estimation of Bursts of Diracs

Let us now consider a sequence of bursts of K Diracs:

$$x(t) = \sum_b \sum_{k=1}^K x_{b,k} \delta(t - \tau_{b,k}), \quad (19)$$

where the amplitudes $x_{b,k}$ in the same burst b have the same sign and satisfy $|x_{b,k}| < 1$.

Proposition 3. *The timing information $t_{1,i}, t_{2,i}, \dots, t_{M,i}$ for $i = 0, 1, \dots, K - 1$ provided by K devices as in Fig. 1 is a sufficient representation of bursts of K Diracs as in Eq. (19), when the reference signal $g(t) = A \cos(\omega_s t)$ has amplitude $A > K$ and period $T_s \leq \frac{2L}{7}$, with L being the support of the sampling kernel $\varphi(t)$. In addition, the spacing between consecutive bursts must be larger than L , and the maximum separation between the last and first Dirac in any burst b should satisfy $\tau_{b,K} - \tau_{b,1} < \frac{T_s}{2}$. The filter $\varphi(t)$ of the m^{th} TEM is a second-order E-spline, which can reproduce two different exponentials, $e^{j\omega_{m_0} t}$ and $e^{j\omega_{m_1} t}$, with $\omega_{m_0} = \omega_0 + \lambda m$, $\lambda = \frac{-2\omega_0}{2K-1}$, $0 < \omega_0 \leq \frac{\pi}{L}$, $\omega_{m_1} = -\omega_{m_0}$, and $m = 0, 1, \dots, K - 1$.*

Proof. See Appendix B. \square

IV. PERFECT RECOVERY FROM TIMING INFORMATION OBTAINED WITH AN INTEGRATE-AND-FIRE TEM

We now shift our focus on the integrate-and-fire TEM in Fig. 3. In particular, we show how to perfectly estimate an input Dirac, and extend this method to streams and bursts of Diracs, streams of pulses as well as piecewise constant signals. The retrieval of these signals from their timing information is perfect, provided the threshold of the trigger comparator is small enough to ensure a sufficient density of output samples. As it will become evident in Section VI, an important feature of the integrate-and-fire model is that it can be more efficient than the comparator or a system based on uniform sampling, in the case of input signals with a small number of Diracs, because it leads to a smaller number of samples.

A. Estimation of an Input Dirac

Proposition 4. *The timing information t_1, t_2, \dots, t_M provided by the integrate-and-fire TEM in Fig. 3 is a sufficient representation of an input Dirac as in Eq. (15) when the sampling kernel is a second-order E-spline of support L , which can reproduce the exponentials $e^{j\omega_0 t}$ and $e^{j\omega_1 t}$, with $0 < \omega_0 \leq \frac{\pi}{L}$ and $\omega_1 = -\omega_0$. Moreover, the trigger mark of the comparator must satisfy:*

$$0 < C_T < \frac{A_{\min}}{3} \int_0^{\frac{L}{2}} \varphi(-t) dt,$$

where A_{\min} is the absolute minimum amplitude of the Dirac.

Proof. First, we note that:

$$\int_0^{\frac{L}{2}} \varphi(-t) dt = \int_{\tau_1}^{\tau_1 + \frac{L}{2}} \varphi(\tau_1 - t) dt \stackrel{(a)}{=} \frac{1}{\omega_0^2} [1 - \cos(\omega_0 \frac{L}{2})], \quad (20)$$

where (a) follows from Eq. (12), given $\alpha_0 = -j\omega_0$, $\alpha_1 = -j\omega_1$ and $\omega_1 = -\omega_0$.

Then, we assume for simplicity that the Dirac's amplitude satisfies $x_1 > 0$ and re-write the upper bound on C_T as:

$$3C_T < A_{\min} \int_0^{\frac{L}{2}} \varphi(-t) < \int_{\tau_1}^{\tau_1 + \frac{L}{2}} x_1 \varphi(\tau_1 - t) dt, \quad (21)$$

where (a) follows from Eq. (20).

Furthermore, from Eq. (2) and (4), we know that:

$$3C_T = \int_{\tau_1}^{t_3} f(t) dt \stackrel{(b)}{=} \int_{\tau_1}^{t_3} x_1 \varphi(\tau_1 - t) dt, \quad (22)$$

where (b) follows from Eq. (3) and given the input signal is $x(t) = x_1 \delta(t - \tau_1)$.

Then, from Eq. (21) and Eq. (22), we obtain the inequality:

$$\int_{\tau_1}^{t_3} x_1 \varphi(\tau_1 - t) dt < \int_{\tau_1}^{\tau_1 + \frac{L}{2}} x_1 \varphi(\tau_1 - t) dt. \quad (23)$$

Using the hypotheses $\omega_0 \leq \frac{\pi}{L}$ and $\omega_1 = -\omega_0$, together with Eq. (12), one can show that $\varphi(\tau_1 - t)$ is positive in the range $[\tau_1, \tau_1 + \frac{L}{2}]$. Hence, from Eq. (23) we get that $t_3 < \tau_1 + \frac{L}{2}$.

As a result, the locations of the first non-uniform output samples satisfy $t_1, t_2, t_3 \in [\tau_1, \tau_1 + \frac{L}{2}]$, and can be computed using Eq. (8) and Eq. (7) as follows:

$$y(t_1) = \int_{\tau_1}^{t_1} f(t) dt = \langle x(t), (\varphi * q_{\theta_1})(t - \tau_1) \rangle,$$

$$y(t_2) = \langle x(t), (\varphi * q_{\theta_2})(t - t_1) \rangle, \quad (24)$$

$$y(t_3) = \langle x(t), (\varphi * q_{\theta_3})(t - t_2) \rangle, \quad (25)$$

for $\theta_1 = t_1 - \tau_1$, $\theta_2 = t_2 - t_1$ and $\theta_3 = t_3 - t_2$.

Furthermore, since $\varphi(t)$ is a second-order E-spline which can reproduce the exponentials $e^{j\omega_0 t}$ and $e^{j\omega_1 t}$ as in Eq. (12), and given the definition of $q_{\theta_n}(t)$ in Eq. (6), we have that:

$$(\varphi * q_{\theta_1})(t - \tau_1) = \frac{1}{\omega_0(\omega_0 - \omega_1)} [(e^{-j\omega_0 t_1} - e^{-j\omega_1 t_1})e^{j\omega_0 t} + (e^{-j\omega_1 t_1} - e^{-j\omega_1 \tau_1})e^{j\omega_1 t}],$$

for $t \in [t_1 - \frac{L}{2}, t_1]$.

Similarly:

$$(\varphi * q_{\theta_2})(t - t_1) = \frac{1}{\omega_0(\omega_0 - \omega_1)} [(e^{-j\omega_0 t_2} - e^{-j\omega_1 t_2})e^{j\omega_0 t} + (e^{-j\omega_1 t_2} - e^{-j\omega_1 t_1})e^{j\omega_1 t}],$$

for $t \in [t_2 - \frac{L}{2}, t_2]$, and

$$(\varphi * q_{\theta_3})(t - t_2) = \frac{1}{\omega_0(\omega_0 - \omega_1)} [(e^{-j\omega_0 t_3} - e^{-j\omega_1 t_3})e^{j\omega_0 t} + (e^{-j\omega_1 t_3} - e^{-j\omega_1 t_2})e^{j\omega_1 t}],$$

for $t \in [t_3 - \frac{L}{2}, t_3]$.

The shifted kernel $(\varphi * q_{\theta_1})(t - \tau_1)$ depends on the Dirac's location τ_1 , and hence its shape cannot be determined a-priori. On the other hand, the shifted kernels $(\varphi * q_{\theta_2})(t - t_1)$ and $(\varphi * q_{\theta_3})(t - t_2)$ are independent of τ_1 and can be written as a linear combination of the exponentials $e^{j\omega_0 t}$ and $e^{j\omega_1 t}$, for $t \in [t_3 - \frac{L}{2}, t_1]$. Therefore, in the interval $I = [t_3 - \frac{L}{2}, t_1]$, where there are no knots of either the shifted kernel $(\varphi * q_{\theta_2})(t - t_1)$ or $(\varphi * q_{\theta_3})(t - t_2)$, we can use the proof in Section II-B2 to find the unique coefficients $c_{m,2}^I$ and $c_{m,3}^I$ such that:

$$\sum_{n=2}^3 c_{m,n}^I (\varphi * q_{\theta_n})(t - t_{n-1}) = e^{j\omega_m t}, \quad (26)$$

for $m \in \{0, 1\}$ and $t \in [t_3 - \frac{L}{2}, t_1]$.

Then, we can define the signal moments as:

$$s_m = \sum_{n=2}^3 c_{m,n}^I y(t_n) \stackrel{(a)}{=} x_1 \sum_{n=2}^3 c_{m,n}^I (\varphi * q_{\theta_n})(\tau_1 - t_{n-1}) \stackrel{(b)}{=} x_1 e^{j\omega_m \tau_1}, \quad \text{for } m \in \{0, 1\}. \quad (27)$$

In the derivations above, (a) follows from Eq. (15), (24) and (25). Moreover, (b) follows from $\tau_1 \in [t_3 - \frac{L}{2}, t_1]$ which is true given Eq. (23), and since the property in Eq. (26) holds within $[t_3 - \frac{L}{2}, t_1]$.

Finally, using Prony's method we can uniquely estimate the input parameters x_1 and τ_1 , from the two signal moments s_m given by Eq. (27), for $m \in \{0, 1\}$ and $\omega_1 = -\omega_0$. \square

B. Estimation of a Stream of Diracs

Proposition 5. *The timing information t_1, t_2, \dots, t_M provided by the integrate-and-fire TEM in Fig. 3 is a sufficient representation of a stream of Diracs as in Eq. (18) when the sampling kernel is a second-order E-spline of support L , which can reproduce the complex exponentials $e^{j\omega_0 t}$ and $e^{j\omega_1 t}$ with $\omega_1 = -\omega_0$ and $0 < \omega_0 \leq \frac{\pi}{T}$. Moreover, the minimum separation between consecutive Diracs is L and the trigger mark of the comparator must satisfy:*

$$0 < C_T < \frac{A_{\min}}{4\omega_0^2} [1 - \cos(\omega_0 \frac{L}{2})], \quad (28)$$

where A_{\min} is the absolute minimum amplitude of any Dirac in the input signal.

Proof. The first Dirac $\delta_1 = x_1 \delta(t - \tau_1)$ can be correctly estimated using the method in Section IV-A, since Eq. (28) satisfies the requirements of Proposition 4. Then, suppose we aim to estimate the second Dirac in the input signal,

and let us assume for simplicity that its amplitude satisfies $x_2 > 0$. Moreover, let us denote the output spike locations in the interval $[\tau_1, \tau_1 + L]$ with t_1, t_2, \dots, t_{n-1} , and the time information after $\tau_1 + L$ with t_n, t_{n+1}, \dots, t_M . Then, given the hypothesis that the minimum separation between consecutive Diracs is L , the location of the second Dirac must satisfy $\tau_2 \in [\tau_1 + L, t_n]$. We also have that:

$$\int_{\tau_2}^{\tau_2 + \frac{L}{2}} f(\tau) d\tau = \int_{\tau_2}^{\tau_2 + \frac{L}{2}} x_2 \varphi(\tau_2 - \tau) d\tau \stackrel{(a)}{=} \frac{x_2}{\omega_0^2} [1 - \cos(\omega_0 \frac{L}{2})],$$

where (a) follows from Eq. (12), for $\omega_1 = -\omega_0$.

This shows the upper bound in Eq. (28) is equivalent to:

$$4C_T < \int_{\tau_2}^{\tau_2 + \frac{L}{2}} f(\tau) d\tau. \quad (29)$$

Furthermore, we have that:

$$\int_{\tau_2}^{t_{n+2}} f(\tau) d\tau = \int_{t_{n-1}}^{t_{n+2}} f(\tau) d\tau - \int_{t_{n-1}}^{\tau_2} f(\tau) d\tau \stackrel{(a)}{=} 3C_T - \int_{t_{n-1}}^{\tau_2} f(\tau) d\tau \stackrel{(b)}{<} 4C_T, \quad (30)$$

where (a) follows from Eq. (2), and (b) holds since t_{n-1} and t_n are consecutive output spikes, and $t_n > \tau_2 > t_{n-1}$.

As a result, Eq. (29) and (30) give the following inequality:

$$\int_{\tau_2}^{t_{n+2}} f(\tau) d\tau < \int_{\tau_2}^{\tau_2 + \frac{L}{2}} f(\tau) d\tau. \quad (31)$$

As shown in Section IV-A, the sampling kernel satisfies $\varphi(t) > 0$ for $x_2 > 0$, within the interval $[\tau_2, \tau_2 + \frac{L}{2}]$. This means that the inequality in Eq. (31) is equivalent to $t_{n+2} < \tau_2 + \frac{L}{2}$, which guarantees that the output samples y_n, y_{n+1} and y_{n+2} occur in the time interval $[\tau_2, \tau_2 + \frac{L}{2}]$. Using the model of Fig. 3, we compute these non-uniform output samples as:

$$y(t_n) = y_n = \int_{t_{n-1}}^{\tau_1 + L} x_1 \varphi(\tau_1 - \tau) d\tau + \int_{\tau_2}^{t_n} x_2 \varphi(\tau_2 - \tau) d\tau,$$

$$y(t_{n+1}) = y_{n+1} = \int_{t_n}^{\tau_2 + \frac{L}{2}} x_2 \varphi(\tau_2 - \tau) d\tau,$$

$$y(t_{n+2}) = y_{n+2} = \int_{t_{n+1}}^{\tau_2 + \frac{L}{2}} x_2 \varphi(\tau_2 - \tau) d\tau.$$

The sample $y(t_n)$ contains information of both δ_1 and δ_2 , and hence cannot be used for estimation of the latter Dirac. On the other hand, since $t_{n+1}, t_{n+2} \in [\tau_2, \tau_2 + \frac{L}{2}]$, we can use the samples y_{n+1} and y_{n+2} to compute the signal moments as in Section IV-A:

$$s_m = c_{m,1} y_{n+1} + c_{m,2} y_{n+2} = x_2 e^{j\omega_m \tau_2}, \quad \text{for } m \in \{0, 1\}.$$

Once δ_2 is estimated from s_m using Prony's method, we use the non-uniform output samples after $\tau_2 + L$, in order to sequentially retrieve the next Diracs in the input signal. \square

The sampling and reconstruction of a stream of $K = 3$ Diracs of minimum absolute amplitude $A_{\min} = 1$ are depicted in Fig. 9. Here, the filter is a second-order E-spline, of support $L = 2$, which can reproduce the exponentials $e^{\pm j \frac{\pi}{3} t}$, and the comparator's trigger mark is $C_T = 0.11$, which satisfies Eq. (28). Fig. 9(b) shows the filtered input and the output of the integrator. The amplitudes and locations of the estimated Diracs are exact to numerical precision. Finally, in Fig. 9(c) we observe that there are no output spikes in a region where the input signal is constant (zero), which leads to small average density of samples.

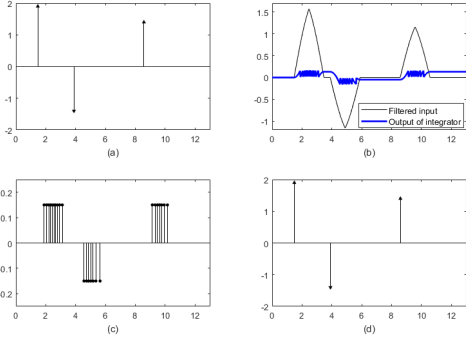


Fig. 9: Sampling of a stream of Diracs using the integrate-and-fire TEM. The input is shown in (a), the filtered input in (b), the output non-uniform samples in (c), and the reconstructed signal in (d).

C. Estimation of a Stream of Pulses

Let us now consider a stream of pulses of the form $x(t) * g(t)$, where $x(t)$ is defined in Eq. (18) and the support of $g(t)$ is $[-\epsilon, \epsilon]$. Filtering this signal with the second-order E-spline $\varphi(t)$ of support L is equivalent to filtering the stream of Diracs $x(t)$ with the modified kernel $(\varphi * g)(t)$. As a case in point, let us consider the cosine-squared pulse $g(t) = \cos^2(t)$, and denote the timing information of the first pulse in the stream $x(t) * g(t)$ with t_1, t_2, \dots, t_M . Then, since $g^{(3)}(t) = -4g^{(1)}(t)$, and assuming $2\epsilon < \frac{L}{2}$ we can leverage the results in Section II-B2 to show that in the knot-free interval $I = [t_5 - \epsilon, t_1 + \epsilon]$, we can perfectly reproduce two exponentials as in Eq. (14), using the shifted kernels $(\varphi * g)(t - t_n)$, for $n = 1, \dots, 5$. We can then compute two signal moments as in Eq. (27), and retrieve the amplitude and location of the first Dirac $x_1 \delta(t - \tau_1)$ in the stream $x(t)$ using Prony's method. In order for these derivations to hold we need to ensure that $\tau_1 \in I$, or in other words that $t_5 < \tau_1 + \epsilon$. Using the same argument as in Section IV-A, the condition $t_5 < \tau_1 + \epsilon$ holds provided the trigger mark of the comparator satisfies $0 < C_T < \frac{A_{min}}{5} \int_{-\epsilon}^{\epsilon} (\varphi * g)(-t) dt$, where $A_{min} = \min(x_1)$.

Finally, once the first pulse has been estimated, and assuming a minimum separation between consecutive pulses of at least $L + 2\epsilon$, we can use subsequent samples after $\tau_1 + L + 2\epsilon$ to retrieve the next pulses in the stream.

The sampling and perfect retrieval of a stream of cosine-squared pulses are depicted in Fig. 10, for $C_T = 0.01$.

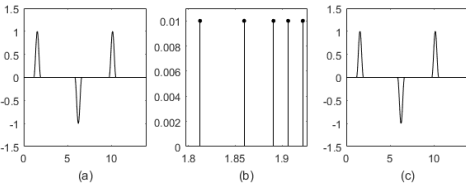


Fig. 10: Sampling of a stream of pulses using the integrate-and-fire TEM. The input is shown in (a), the non-uniform samples used for retrieval of the first pulse in (b), and the reconstructed signal in (c).

D. Multi-channel Estimation of Bursts of Diracs

Let us now consider the estimation of a sequence of bursts of Diracs as in Eq. (19). This problem is equivalent to the estimation of a stream of Diracs, however, this time, the K Diracs can be arbitrarily close to each other. Therefore, the estimation of a burst of K Diracs involves retrieving a larger number of moments (at least $2K$) to accurately retrieve the

Diracs. We employ a multi-channel scheme of K different acquisition devices, each of which will help us compute 2 different signal moments.

Proposition 6. *The timing information $t_{1,i}, t_{2,i}, \dots, t_{M,i}$ for $i = 0, 1, \dots, K - 1$ provided by K devices as in Fig. 3 is a sufficient representation of bursts of K Diracs as in Eq. (19) when the sampling kernel of the m^{th} time encoding machine is a second-order E-spline of support L , which can reproduce the exponentials $e^{j\omega_{m_0}t}$ and $e^{j\omega_{m_1}t}$ with $\omega_{m_1} = -\omega_{m_0}$ and $0 < \omega_{m_0} \leq \frac{\pi}{L}$. Moreover, the spacing between bursts should be larger than L , and the separation between the last and first Diracs within any burst b must satisfy $\tau_{b,K} - \tau_{b,1} < \frac{L}{2}$. In addition, the comparator's trigger mark C_T must satisfy the following conditions for each device m and burst b :*

$$C_T > \frac{(K-1)A_{max}}{\omega_{m_0}^2} [1 - \cos(\omega_{m_0}(\tau_{b,K} - \tau_{b,1}))], \quad (32)$$

$$C_T < \frac{KA_{min}}{5\omega_{m_0}^2} [1 - \cos(\omega_{m_0}(\frac{L}{2} - (\tau_{b,K} - \tau_{b,1})))], \quad (33)$$

where A_{max} and A_{min} are the absolute maximum and minimum amplitudes of the input, and $\tau_{b,1}$ and $\tau_{b,K}$ are the locations of the first and last Diracs in burst b , respectively.

Proof. See Appendix C. \square

Even though we considered the sampling of bursts of Diracs using a multi-channel system, it is possible under slightly more restrictive conditions, to achieve the same using a single TEM device. Therefore, for the sake of completeness, we state the following result without proof:

Proposition 7. *The timing information t_1, t_2, \dots, t_M provided by the device in Fig. 3 is a sufficient representation of a sequence of bursts of K Diracs as in Eq. (19) when the sampling kernel $\varphi_P(t)$ is an E-spline of order $P \geq 2K$ and support L , which can reproduce P different exponentials $e^{j\omega_m t}$, with $\omega_m = \omega_0 + m\lambda$, $m = 0, 1, \dots, P - 1$, and $0 < \omega_0 \leq \frac{\pi}{L}$. In addition, setting P even and $\lambda = \frac{\pi}{P}$ ensures $\varphi(t)$ is a real-valued function. In this setting, the spacing between bursts should be larger than L , and the separation between the last and first Diracs within any burst b must satisfy $\tau_{b,K} - \tau_{b,1} < \frac{L}{P}$. In addition, the trigger mark of the comparator C_T must satisfy the following conditions:*

$$C_T > (K-1)A_{max} \int_0^{\Delta_b} \varphi(-\tau) d\tau, \quad (34)$$

$$C_T < \frac{KA_{min}}{P+3} \int_0^{\frac{L}{P}} \varphi(-\tau) d\tau, \quad (35)$$

where $\Delta_b = \max(\tau_{b,K} - \tau_{b,1})$.

E. Estimation of Piecewise Constant Signals

Let us now consider an input piecewise constant signal $x(t)$, and assume that we filter this with the derivative of an E-spline $\varphi(t)$ of order $P \geq 2$, obtained using Eq. (11). Filtering $x(t)$ with $\frac{d\varphi(t)}{dt}$ ensures that in a region where the input is constant, there are no output spikes, since $\frac{d\varphi(t)}{dt}$ has average value equal to zero. This leads to energy-efficient sampling of the piecewise constant signal, resulting in a small average number of output spikes. In this setting, the filtered input is given by:

$$f(t) = x(t) * \frac{d\varphi(t)}{dt} = \frac{dx(t)}{dt} * \varphi(t).$$

This shows that filtering a piecewise constant signal $x(t)$ with $\frac{d\varphi(t)}{dt}$ is equivalent to filtering the stream of Diracs corresponding to the discontinuities of the piecewise constant

signal with the E-spline $\varphi(t)$. The discontinuities $\frac{dx(t)}{dt}$ can be estimated from the output spikes, by extending the results of Proposition 5 to the case of a P -order E-spline $\varphi_P(t)$, with $P \geq 2$. In this case, the E-spline $\varphi_P(t)$ of support L can reproduce $P \geq 2$ different complex exponentials $e^{j\omega_m t}$, with $\omega_m = \omega_0 + \lambda m$, and $m = 0, 1, \dots, P-1$. Moreover, choosing $\lambda = \frac{-2\omega_0}{P-1}$ and P even ensures the kernel $\varphi_P(t)$ is a real-valued function. As before, the separation between consecutive Diracs must be larger than L and the trigger mark of the comparator must satisfy:

$$0 < C_T < \frac{A_{\min}}{P+2} \int_0^{\frac{L}{P}} \varphi_P(-\tau) d\tau. \quad (36)$$

Suppose we wanted to estimate the k^{th} discontinuity in the signal $\frac{dx(t)}{dt}$, of amplitude z_k and located at τ_k , and let us denote the locations of the first output spikes after τ_k with t_n, t_{n+1}, \dots, t_M . Then, using a similar proof as in Section IV-B, we can show that the constraint in Eq. (36) guarantees that $\tau_k \in I = [t_{n+P} - \frac{L}{P}, t_n]$. Then, we can compute the following signal moments:

$$\begin{aligned} s_m &= \sum_{i=1}^P c_{m,n}^I y(t_{n+i}) \stackrel{(a)}{=} z_k \sum_{i=1}^P c_{m,n}^I (\varphi_P * q_{\theta_{n+i}})(\tau_k - t_{n+i-1}) \\ &\stackrel{(b)}{=} z_k e^{j\omega_m \tau_k}, \text{ for } m = 0, 1, \dots, P-1. \end{aligned}$$

In these derivations, (a) follows from Eq. (7), and (b) holds given $\tau_k \in [t_{n+P} - \frac{L}{P}, t_n]$, and the fact that none of the kernels $(\varphi_P * q_{\theta_{n+i}})(\tau_k - t_{n+i-1})$ have any discontinuities in $[t_{n+P} - \frac{L}{P}, t_n]$, for $i = 1, 2, \dots, P$. As before, we can use Prony's method to estimate z_k and τ_k from the signal moments s_m . Finally, we can retrieve the piecewise constant signal $x(t)$ once we have estimated its discontinuities $\frac{dx(t)}{dt}$.

The sampling and reconstruction of a piecewise constant signal are depicted in Fig. 11. The filter is the derivative of the fourth-order E-spline, of support $L = 4$, as seen in Fig. 11(b), the separation between input discontinuities is larger than the kernel's support L , as depicted in Fig. 11(a), and the comparator's trigger mark is $C_T = 0.001$. The estimation of the input is exact to numerical precision.

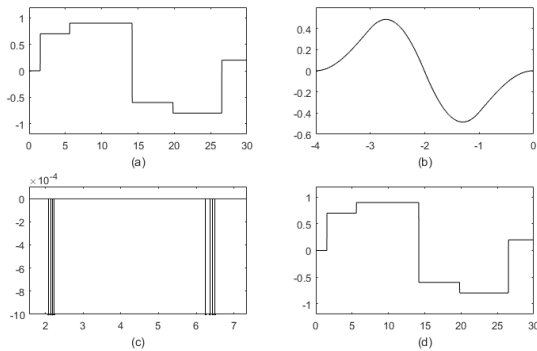


Fig. 11: Sampling of a piecewise constant signal using the integrate-and-fire TEM. The input is shown in (a), the sampling kernel in (b), the non-uniform samples used for estimation of the first two input discontinuities in (c), and the reconstructed signal in (d).

V. GENERALIZED TIME-BASED SAMPLING

To highlight the potential practical implications of the methods developed in the previous sections, we present here extensions of our framework to deal with arbitrary kernels and the noisy scenario, and show that reliable input reconstruction can be achieved also in these scenarios.

A. Sampling with Arbitrary Kernels

In the previous sections we have presented methods for perfect retrieval of certain classes of non-bandlimited signals from timing information. We have seen that these methods require the sampling kernel $\varphi(t)$ to locally reproduce exponentials, in order to be able to map this problem to Prony's method. In reality, however, the sampling kernel may not have the exponential reproducing property as in Eq. (13). Let us now consider an arbitrary kernel $\tilde{\varphi}(t)$, and find a linear combination of its non-uniform shifted versions that gives the best approximation of P exponentials $f(t) = e^{j\omega_m t}$ within an interval I , for $\omega_m = \omega_0 + \lambda m$, $m = 0, 1, \dots, P-1$, and $\lambda = \frac{-2\omega_0}{P-1}$. In other words, we want to find the optimal coefficients $c_{m,n}^I$ such that:

$$\sum_{n=1}^N c_{m,n}^I \tilde{\varphi}(t - t_n) \approx e^{j\omega_m t}, \quad (37)$$

for $t \in I$ and $n = 1, 2, \dots, N$, with N being the number of kernels $\tilde{\varphi}(t - t_n)$ overlapping I .

We find the coefficients $c_{m,n}$ using the *least-squares approximation* method described in [38]. The coefficients are computed using the orthogonal projection of $f(t)$ onto the space spanned by the non-uniform shifts $\tilde{\varphi}(t - t_n)$, such that:

$$\langle f(t) - \sum_{k=1}^N c_{m,k}^I \tilde{\varphi}(t - t_k), \tilde{\varphi}(t - t_n) \rangle = 0, \quad (38)$$

for $t \in I$ and $n = 1, 2, \dots, N$.

Furthermore, Eq. (38) is equivalent to:

$$\langle f(t), \tilde{\varphi}(t - t_n) \rangle = \sum_{k=1}^N c_{m,k}^I \langle \tilde{\varphi}(t - t_k), \tilde{\varphi}(t - t_n) \rangle,$$

which represents a system of N equations from which we can determine the N coefficients $c_{m,k}^I$, for each $m = 0, 1, \dots, P-1$.

We then use the calculated coefficients $c_{m,k}^I$ to compute the signal moments as in Section IV. Finally, the estimation of the input can be further refined using the Cadzow iterative algorithm in order to increase the accuracy of the signal moments, before applying Prony's method [39], [40].

The sampling and reconstruction of bursts of 2 Diracs are depicted in Fig. 13. We use the multi-channel estimation method presented in Section IV-D, where the filter of each channel is a third order B-spline $\beta_3(t)$, such that the modified kernel $(\beta_3 * q_{\theta_n})(t)$ in Eq. (5) cannot reproduce exponentials. Moreover, we aim to approximately reproduce 4 different exponentials for each channel, and hence we require a number of 4 non-uniform samples, as discussed in Section II-B. In Fig. 12, we depict the approximate exponential reproduction in Eq. (37), within the interval $I = [0.82, 1.4]$ overlapping the first burst of Diracs. Finally, the estimation of the input is close to exact, as depicted in Fig. 13(c).

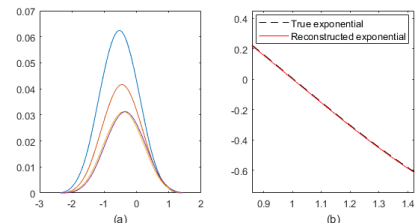


Fig. 12: Approximate exponential reproduction using non-uniform shifts of the kernel $(\beta_3 * q_{\theta_n})(t)$. The kernels are shown in (a), and the exponential reproduction using these shifted kernels in (b).

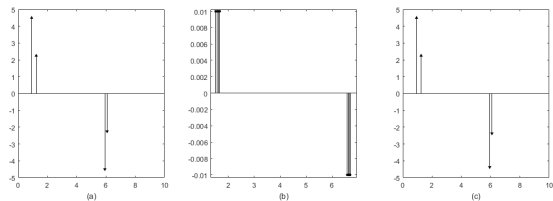


Fig. 13: Universal sampling of a sequence of bursts of Diracs using the integrate-and-fire TEM. The input signal is shown in (a), the output non-uniform samples of one channel used for estimation in (b), and the reconstructed signal in (c).

B. Robustness of the Integrate-and-fire TEM to Noise

In many practical circumstances, the input signal is corrupted by noise, which is typically assumed to be white, additive Gaussian noise. When this happens, the non-uniform times $\{t_n\}$ change which means that the sequence of moments s_m is also corrupted, and perfect reconstruction may no longer be possible. Suppose we filter the noisy input with $h(t)$ to obtain:

$$\begin{aligned} f(t) &= \int_{-\infty}^{+\infty} [x(\tau) + e(\tau)]h(t - \tau)d\tau \\ &= \int_t^{t+L} x(\tau)h(t - \tau)d\tau + \int_t^{t+L} e(\tau)h(t - \tau)d\tau \\ &\stackrel{(a)}{\approx} \int_t^{t+L} x(\tau)h(t - \tau)d\tau, \end{aligned}$$

where $e(t)$ is white Gaussian noise, and (a) holds assuming $e(t)$ has average value equal to 0 and L is sufficiently large.

In Fig. 14 we show the reconstruction of a piecewise constant signal corrupted by white, additive Gaussian noise, using the method in Section IV-E. The filter is the derivative of a fourth-order E-spline of support $L = 4$ which can reproduce the exponentials $e^{\pm j\frac{\pi}{8}t}$ and $e^{\pm j\frac{3\pi}{8}t}$, the trigger mark of the comparator is $C_T = 0.001$, the standard deviation of the noise is $\sigma = 0.1$ (SNR = 21.56dB), and the separation between consecutive discontinuities of the input is larger than L . The reconstruction of the input from noisy samples is very accurate. A quantitative analysis of the effect of noise on the retrieval of this piecewise constant signal is presented in Table I. The table shows the error of the estimated locations and the relative error of the estimated amplitudes of the discontinuities in the input signal, averaged over 10000 experiments.

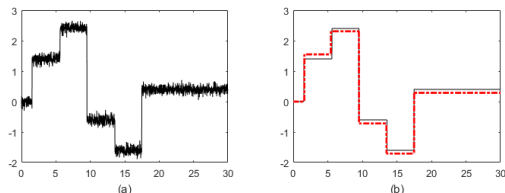


Fig. 14: Estimation of a piecewise constant signal from noisy samples, obtained using the integrate-and-fire TEM. The noisy input is shown in (a), and the reconstruction in (b).

VI. DENSITY OF NON-UNIFORM SAMPLES OBTAINED WITH AN INTEGRATE-AND-FIRE TEM

In the previous sections, we have presented techniques for estimation of non-bandlimited signals from timing information. We have seen that perfect estimation can be achieved using simple algorithms, and physically realisable kernels. In this section we outline the fact that in many settings sampling

TABLE I: Effect of noise on the estimation of a piecewise constant signal, from spikes obtained using the integrate-and-fire TEM. The error ϵ_t is the average absolute difference between the true and estimated locations, and ϵ_A is the relative error of the estimated amplitudes of the input discontinuities.

σ	ϵ_t	ϵ_A
0.01	2.61×10^{-4}	6.21×10^{-5}
0.05	0.0015	2.1509×10^{-4}
0.1	0.0042	0.0026

based on timing using our integrate-and-fire system is an efficient way to acquire signals, resulting in a smaller density of samples, compared to classical sampling.

As a case in point we consider the retrieval of bursts of K Diracs, described in Section IV-D. We have seen that perfect reconstruction from timing information can be achieved, provided the separation between consecutive bursts is at least L , and that the Diracs within any burst are sufficiently close. In particular, let us denote the maximum separation between the last and first Dirac within a burst with $\Delta = \max(\tau_K - \tau_1) < \frac{L}{2}$, which can be determined according to Eq. (32) and (33). Moreover, let us assume the input is sufficiently sparse, such that the average separation between consecutive bursts is $L+S$, with $S > 0$. Under these assumptions, the results in [6] show that in order to retrieve the K Diracs from uniform samples, we need at least $2K$ samples within the interval $L - \Delta$ following the burst of Diracs. As a result, the uniform sampling period must satisfy $T \leq \frac{L-\Delta}{2K}$. Then, the number of uniform samples we record within an interval of length $L + S$ is $\frac{L+S}{T} = \frac{2K(L+S)}{L-\Delta}$. On the other hand, in the case of time encoding using the integrate-and-fire TEM in Fig. 3, the results in Section IV-D show that we need to record 4 output samples for each of the K channels (or equivalently, $4K$ samples for the case of single-channel sampling), for each burst of K Diracs. We note that Eq. (33) shows that in many situations, the TEM outputs more than 4 spikes per channel. Nevertheless, these samples can be discarded since they are not used in estimation. For example, one way to stop recording spikes once we have obtained 4 non-zero samples, is to increase the trigger mark C_T of the comparator in Fig. 3, for a duration of $L - \Delta$.

Moreover, when the input is constant (zero), the integrate-and-fire TEM does not fire, and hence there are no output samples. Therefore, in an interval of size $L + S$, the number of stored samples from a K -Dirac burst is $4K$, $\forall S$.

Furthermore, $\frac{2K(L+S)}{L-\Delta} > 4K$ for $S \geq L - 2\Delta > 0$ and $\forall K$, which shows that the average number of non-uniform spikes required for the retrieval of K Diracs is lower than the number of uniform samples required to estimate the same number of free input parameters, when the input is sufficiently sparse.

VII. CONCLUSIONS

In this work we established time encoding as an alternative sampling method for some classes of non-bandlimited signals. The proposed sampling scheme is based on first filtering the input signal, before retrieving the timing information using a crossing or integrate-and-fire TEM. We demonstrated sufficient conditions for the exact recovery of streams of

Diracs, streams of pulses and piecewise constant signals, from their time-based samples. Central to our reconstruction methods is the use of specific filters that we proved can locally reproduce polynomials or exponentials. We further highlighted the potential of this new framework by showing that it is resilient to noise and that it can handle non-ideal filters.

APPENDIX A PRONY'S METHOD

One way to solve the problem of estimating the parameters $\{b_k, u_k\}_{k=1}^K$ from the sequence $s_m = \sum_{k=1}^K b_k u_k^m$ is given by the annihilating filter method, also referred to as Prony's method [32]. The name of this approach comes from the observation that if we filter s_m with a filter which has zeros at $\{u_k\}_{k=1}^K$, the output is zero, or in other words, this filter annihilates the sequence s_m .

The z-transform of the annihilating filter satisfies:

$$H(z) = \sum_{m=0}^K h_m z^{-m} = \prod_{k=1}^K (1 - u_k z^{-1}), \quad (39)$$

which evaluates to zero when $z = u_k$.

Filtering the sequence s_m with h_m corresponds to the convolution of these sequences:

$$h_m * s_m = \sum_{l=0}^K h_l s_{m-l} = \sum_{k=1}^K b_k u_k^m \sum_{l=0}^K h_l u_k^{-l} \stackrel{(a)}{=} 0, \quad (40)$$

where (a) holds since $z = u_k$ gives $H(z) = 0$ in Eq. (39).

Eq. (40) can be written in matricial form as follows:

$$\begin{bmatrix} s_K & s_{K-1} & \cdots & s_0 \\ s_{K+1} & s_K & \cdots & s_1 \\ \vdots & \vdots & \ddots & \vdots \\ s_{2K-1} & s_{2K-2} & \cdots & s_{K-1} \end{bmatrix} \begin{bmatrix} 1 \\ h_1 \\ \vdots \\ h_K \end{bmatrix} = \mathbf{S} \mathbf{h} = 0. \quad (41)$$

It can be shown that provided $\{b_k\}_{k=1}^K$ are non-zero and $\{u_k\}_{k=1}^K$ are distinct, matrix \mathbf{S} has full row rank K , which means the solution \mathbf{h} given by Eq. (41) is unique. Moreover, the solution \mathbf{h} can be obtained by performing a singular value decomposition of \mathbf{S} , where \mathbf{h} is the singular vector corresponding to the zero singular value.

Then, once the coefficients h_m of the polynomial $H(z)$ are known, the parameters $\{u_k\}_{k=1}^K$ are obtained from the roots of this filter. Finally, once $\{u_k\}_{k=1}^K$ are found, the parameters $\{b_k\}_{k=1}^K$ can be computed from the linear system of K equations given by $s_m = \sum_{k=1}^K b_k u_k^m$, with $m = 0, 1, \dots, K-1$.

APPENDIX B

A. Proof of Proposition 3

Suppose we want to estimate the Diracs in the first burst, located at $\tau_{1,1}, \dots, \tau_{1,K}$. Moreover, assume for simplicity that their amplitudes satisfy $x_{1,1}, \dots, x_{1,K} > 0$. In addition, let us consider the output of the m^{th} TEM device, and denote its timing information with $\{t_1, t_2, \dots, t_M\}$.

Since we assume all the amplitudes in the first burst satisfy $0 < x_{1,k} < 1$, and since $0 \leq \varphi(t) < 1$, we get $0 \leq y(t)$ and $y(t) = \sum_{k=1}^K x_k \varphi(\tau_k - t) < K < A = \max(g(t))$.

Then, Bolzano's intermediate value theorem [36] guarantees that the m^{th} TEM outputs at most one sample in the interval $[\tau_{1,1}, \tau_{1,K}]$, given the assumption $\tau_{1,K} - \tau_{1,1} < \frac{T_s}{2}$, and the fact that $0 \leq y(t) < \max(g(t))$. At the same time, this theorem also guarantees that the filtered input $y(t)$ crosses

the sinusoidal reference signal in at least 3 points, within the window $[\tau_{1,1}, \tau_{1,1} + \frac{7T_s}{4}]$, such that $t_3 - \tau_{1,1} \leq \frac{7T_s}{4}$. Moreover, the assumption $T_s \leq \frac{2L}{7}$ ensures that $t_3 - \tau_{1,1} \leq \frac{L}{2}$. Hence, whilst the spike at t_1 may occur before $\tau_{1,K}$, the second and third spikes satisfy $t_2, t_3 \in [\tau_{1,K}, \tau_{1,1} + \frac{L}{2}]$, which means that $\tau_{1,1}, \tau_{1,2}, \dots, \tau_{1,K} \in [t_3 - \frac{L}{2}, t_2]$.

Since in the interval $I = [t_3 - \frac{L}{2}, t_2]$ there are no discontinuities of either $\varphi(t - t_2)$ or $\varphi(t - t_3)$, we can compute the following signal moments for the m^{th} channel:

$$\begin{aligned} s_{m_i} &= \sum_{n=2}^3 c_{m_i, n}^I y(t_n) \stackrel{(a)}{=} \sum_{n=2}^3 c_{m_i, n}^I \langle x(t), \varphi(t - t_n) \rangle \\ &\stackrel{(b)}{=} \int_{-\infty}^{\infty} x(t) \sum_{n=2}^3 c_{m_i, n}^I \varphi(t - t_n) dt \stackrel{(c)}{=} \int_{-\infty}^{\infty} x(t) e^{j\omega_{m_i} t} dt \\ &\stackrel{(d)}{=} \int_I \sum_{k=1}^K x_{1,k} \delta(t - \tau_{1,k}) e^{j\omega_{m_i} t} dt = \sum_{k=1}^K x_{1,k} e^{j\omega_{m_i} \tau_{1,k}}. \end{aligned}$$

where $i \in \{0, 1\}$, and $\omega_{m_i} = \omega_0 + \lambda m_i$, with $m_0 = m$ and $m_1 = 2K - 1 - m$ (which ensures $\omega_{m_0} = -\omega_{m_1}$).

In the derivations above, (a) follows from Eq. (1), (b) from the linearity of the inner product, and (c) from the local exponential reproduction property of the sampling kernel described in Eq. (13), for $N = 2$. Moreover, (d) follows from Eq. (19), and given that $\tau_{1,1}, \tau_{1,2}, \dots, \tau_{1,K} \in [t_3 - \frac{L}{2}, t_1]$.

By using the same approach on each of the K channels, we can retrieve $2K$ different moments and, due to the specific choice of exponents, the $2K$ moments can be expressed as:

$$s_m = \sum_{k=1}^K x_{1,k} e^{j\omega_0 \tau_{1,k}} e^{j\lambda m \tau_{1,k}} = \sum_{k=1}^K b_k u_k^m,$$

where $b_k = e^{j\omega_0 \tau_{1,k}}$, $u_k = e^{j\lambda \tau_{1,k}}$, and $m = 0, 1, \dots, 2K - 1$.

We can then apply Prony's method on s_m to retrieve the K amplitudes and the K locations of the Diracs. Finally, we use subsequent output samples, located after $\tau_{1,K} + L$ to retrieve the free parameters of the Diracs in the second burst, and we reiterate the process for the following bursts.

The sampling and reconstruction of a sequence of bursts of 2 Diracs are depicted in Fig. 15. Here, the sampling kernel is a second-order E-spline for each channel, of support $L = 2$, shown in Fig. 15(c) and (d). The first channel's kernel reproduces the exponentials $e^{\pm j \frac{\pi}{3} t}$, whereas the second kernel reproduces $e^{\pm j \frac{\pi}{9} t}$. Moreover, the comparator's reference signal has frequency $f_s = 1.76 > \frac{7}{2L}$, and the separation between consecutive bursts of Diracs is at least L . The amplitudes and locations of the estimated Diracs are exact.

APPENDIX C

A. Proof of Proposition 6

Let us assume we want to retrieve burst b and denote with t_n, t_{n+1}, \dots, t_M the output spikes located after $\tau_{b-1,K} + L$. Then we have that $t_n > \tau_{b,1} > t_{n-1}$, where $\tau_{b,1}$ is the location of the first Dirac in the b^{th} burst. Furthermore, let us assume for simplicity that the Diracs in the b^{th} burst satisfy $x_{b,1}, \dots, x_{b,K} > 0$, as depicted in Fig. 16.

In what follows, we show that the samples $y(t_{n+2})$ and $y(t_{n+3})$ can be reliably used to estimate the b^{th} burst.

We first prove that the following conditions hold:

$$t_{n+1} > \tau_{b,K}, \quad (42)$$

and:

$$t_{n+3} < \tau_{b,1} + \frac{L}{2}. \quad (43)$$

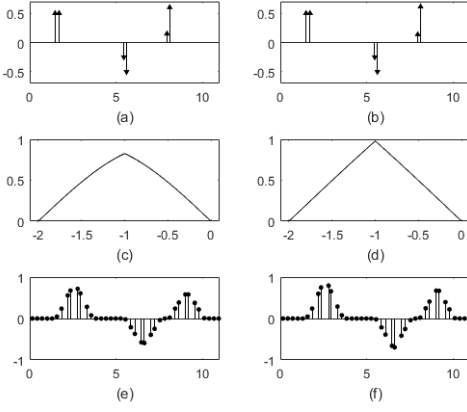


Fig. 15: Sampling of bursts of Diracs using the crossing TEM. The input signal is shown in (a), the reconstructed signal in (b), the sampling kernels of both channels in (c) and (d) respectively, and the corresponding non-uniform samples in (e) and (f).

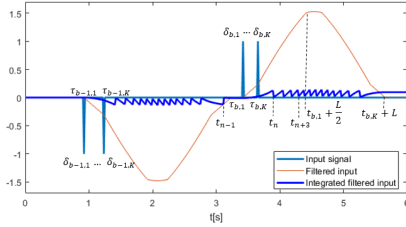


Fig. 16: Time encoding of a sequence of 2 bursts of 2 Diracs.

We note that since we assume $x_{b,1}, \dots, x_{b,K} > 0$, the filtered input defined in Eq. (3) satisfies $f(\tau) > 0$, and hence the condition in Eq. (42) is equivalent to:

$$\int_{\tau_{b,1}}^{t_{n+1}} f(\tau) d\tau > \int_{\tau_{b,1}}^{\tau_{b,K}} f(\tau) d\tau. \quad (44)$$

The left-hand side of this inequality can be expressed as:

$$\begin{aligned} \int_{\tau_{b,1}}^{t_{n+1}} f(\tau) d\tau &= \int_{t_{n-1}}^{t_{n+1}} f(\tau) d\tau - \int_{t_{n-1}}^{\tau_{b,1}} f(\tau) d\tau \\ &\stackrel{(a)}{=} 2C_T - \int_{t_{n-1}}^{\tau_{b,1}} f(\tau) d\tau \stackrel{(b)}{>} C_T, \end{aligned} \quad (45)$$

where (a) holds given Eq. (2) and (b) since $t_n > \tau_{b,1} > t_{n-1}$. The right-hand side of Eq. (44) can be re-written as:

$$\begin{aligned} \int_{\tau_{b,1}}^{\tau_{b,K}} f(\tau) d\tau &\stackrel{(a)}{=} \sum_{k=1}^{K-1} \int_{\tau_{b,k}}^{\tau_{b,K}} x_{b,k} \varphi(\tau_{b,k} - \tau) d\tau \\ &\stackrel{(b)}{<} \sum_{k=1}^{K-1} A_{max} \int_{\tau_{b,k}}^{\tau_{b,K}} \varphi(\tau_{b,k} - \tau) d\tau \\ &\stackrel{(c)}{<} \frac{(K-1)A_{max}}{\omega_{m_0}^2} [1 - \cos(\omega_{m_0}(\tau_{b,K} - \tau_{b,1}))] \\ &\stackrel{(d)}{<} C_T \stackrel{(e)}{<} \int_{\tau_{b,1}}^{t_{n+1}} f(\tau) d\tau, \end{aligned}$$

which proves the inequality in Eq. (42).

In the derivations above, (a) follows from the definition in Eq. (3), and (b) holds since we assume $x_{b,1}, \dots, x_{b,K} > 0$. In addition, (d) follows from Eq. (32) and (e) from Eq. (45). Finally, condition (c) follows from:

$$\begin{aligned} \int_{\tau_{b,k}}^{\tau_{b,K}} \varphi(\tau_{b,k} - \tau) d\tau &\stackrel{(a)}{=} \frac{1}{\omega_{m_0}^2} [1 - \cos(\omega_{m_0}(\tau_{b,K} - \tau_{b,k}))] \\ &\stackrel{(b)}{<} \frac{1}{\omega_{m_0}^2} [1 - \cos(\omega_{m_0}(\tau_{b,K} - \tau_{b,1}))]. \end{aligned}$$

where (a) follows from the definition of $\varphi(\tau_{b,k} - \tau)$ in Eq. (12) for $\tau \in [\tau_{b,k}, \tau_{b,K}]$ with $\tau_{b,K} < \tau_{b,k} + \frac{L}{2}$, and from the hypothesis that $\varphi(\tau)$ reproduces the exponentials $e^{\pm j\omega_{m_0}\tau}$. Moreover, (b) follows from the hypothesis that $0 < \omega_{m_0} \leq \frac{\pi}{L}$ which is equivalent to $0 < \frac{\omega_{m_0}L}{2} \leq \frac{\pi}{2}$, and from the assumption that $\tau_{b,K} - \tau_{b,k} < \frac{L}{2}$, which means that $0 < \omega_{m_0}(\tau_{b,K} - \tau_{b,k}) < \frac{\pi}{2}$, and hence $1 - \cos(\omega_{m_0}(\tau_{b,K} - \tau_{b,1})) > 1 - \cos(\omega_{m_0}(\tau_{b,K} - \tau_{b,k})) \forall k = 2, \dots, K$.

Similarly, since $f(\tau) > 0$ for $x_{b,1}, \dots, x_{b,K} > 0$, Eq. (43) is equivalent to:

$$\int_{\tau_{b,1}}^{\tau_{b,1} + \frac{L}{2}} f(\tau) d\tau > \int_{\tau_{b,1}}^{t_{n+3}} f(\tau) d\tau, \quad (46)$$

where the left-hand side can be expressed as:

$$\begin{aligned} \int_{\tau_{b,1}}^{\tau_{b,1} + \frac{L}{2}} f(\tau) d\tau &\stackrel{(a)}{=} \sum_{k=1}^K \int_{\tau_{b,k}}^{\tau_{b,1} + \frac{L}{2}} x_k \varphi(\tau_{b,k} - \tau) d\tau \\ &\stackrel{(b)}{=} \frac{1}{\omega_{m_0}^2} \sum_{k=1}^K x_{b,k} [1 - \cos(\omega_{m_0}(\frac{L}{2} - (\tau_{b,k} - \tau_{b,1})))] \\ &\stackrel{(c)}{>} \frac{1}{\omega_{m_0}^2} \sum_{k=1}^K x_{b,k} [1 - \cos(\omega_{m_0}(\frac{L}{2} - (\tau_{b,K} - \tau_{b,1})))] \\ &\stackrel{(d)}{>} \frac{KA_{min}}{\omega_{m_0}^2} [1 - \cos(\omega_{m_0}(\frac{L}{2} - (\tau_{b,K} - \tau_{b,1})))] \stackrel{(e)}{>} 5C_T, \end{aligned} \quad (47)$$

where (a) follows from Eq. (3), (b) follows from the definition of $\varphi(\tau_{b,k} - \tau)$ in Eq. (12) for $\tau \in [\tau_{b,k}, \tau_{b,1} + \frac{L}{2}]$, and (c) follows from the hypothesis that $0 < \omega_{m_0} \leq \frac{\pi}{L}$ which is equivalent to $0 < \frac{\omega_{m_0}L}{2} \leq \frac{\pi}{2}$, and since $\tau_{b,k} - \tau_{b,1} < \frac{L}{2} \forall k = 2, \dots, K$. Moreover, (d) holds since we assume $x_{b,1}, \dots, x_{b,K} > 0$, and (e) follows from Eq. (33).

Finally, the right-hand side of Eq. (46) is equivalent to:

$$\begin{aligned} \int_{\tau_{b,1}}^{t_{n+3}} f(\tau) d\tau &= \int_{t_{n-1}}^{t_{n+3}} f(\tau) d\tau - \int_{t_{n-1}}^{\tau_{b,1}} f(\tau) d\tau \\ &\stackrel{(a)}{=} 4C_T - \int_{t_{n-1}}^{\tau_{b,1}} f(\tau) d\tau \\ &\stackrel{(b)}{<} 4C_T - (-C_T) \stackrel{(c)}{=} 5C_T < \int_{\tau_{b,1}}^{\tau_{b,1} + \frac{L}{2}} f(\tau) d\tau, \end{aligned}$$

hence proving the result in Eq. (43).

In these derivations, (a) follows from Eq. (2), (b) holds since $t_n > \tau_{b,1} > t_{n-1}$ and (c) follows from Eq. (47).

The conditions in Eq. (42) and (43) ensure that the output samples $y(t_{n+2})$ and $y(t_{n+3})$ have contributions only from all the Diracs in the b^{th} burst. These samples can be computed using Eq. (5) for each channel m , as follows:

$$\begin{aligned} y(t_{n+2}) &= \langle x(t), (\varphi * q_{\theta_{n+2}})(t - t_{n+1}) \rangle \\ &\stackrel{(a)}{=} \sum_{k=1}^K x_{b,k} (\varphi * q_{\theta_{n+2}})(\tau_{b,k} - t_{n+1}), \end{aligned} \quad (48)$$

where $\theta_{n+2} = t_{n+2} - t_{n+1}$, and derivation (a) follows from the definition in Eq. (19). Similarly, we can write $y(t_{n+3})$ as:

$$y(t_{n+3}) = \sum_{k=1}^K x_{b,k} (\varphi * q_{\theta_{n+3}})(\tau_{b,k} - t_{n+2}), \quad (49)$$

where $\theta_{n+3} = t_{n+3} - t_{n+2}$.

For each channel m , the signal $(\varphi * q_{\theta_{n+2}})(t - t_{n+1})$ is a linear combination of the exponentials $e^{j\omega_{m_0}t}$ and $e^{j\omega_{m_1}t}$, for $t \in [t_{n+2} - \frac{L}{2}, t_{n+1}]$, given Eq. (12) and Eq. (6). Similarly, $(\varphi * q_{\theta_{n+3}})(t - t_{n+2})$ is a linear combination of the exponentials $e^{j\omega_{m_0}t}$ and $e^{j\omega_{m_1}t}$, for $t \in [t_{n+3} - \frac{L}{2}, t_{n+1}]$. Therefore, in the interval $[t_{n+3} - \frac{L}{2}, t_{n+1}]$, where there are no knots of either

$(\varphi * q_{\theta_{n+2}})(t - t_{n+1})$ or $(\varphi * q_{\theta_{n+3}})(t - t_{n+2})$, we use the proof in Section II-B2 to find unique $c_{m_i,2}$ and $c_{m_i,3}$ such that:

$$c_{m_i,2}(\varphi * q_{\theta_{n+2}})(t - t_{n+1}) + c_{m_i,3}(\varphi * q_{\theta_{n+3}})(t - t_{n+2}) = e^{j\omega_{m_i} t}, \quad (50)$$

for $i \in \{0, 1\}$, $t \in [t_{n+3} - \frac{L}{2}, t_{n+1}]$, $m_0 = m$ and $m_1 = 2K - 1 - m$ (which ensures $\omega_{m_1} = -\omega_{m_0}$).

Then, for each channel m we can compute the signal moments as before:

$$s_{m_i} = c_{m_i,2}y(t_{n+2}) + c_{m_i,3}y(t_{n+3})$$

$$\stackrel{(a)}{=} \sum_{k=1}^K x_{b,k} \sum_{l=n+2}^{n+3} c_{m_i,l}(\varphi * q_{\theta_l})(\tau_{b,k} - t_{l-1}) \stackrel{(b)}{=} \sum_{k=1}^K x_{b,k} e^{j\omega_{m_i} \tau_{b,k}},$$

where $i \in \{0, 1\}$, $m_0 = m$ and $m_1 = 2K - 1 - m$.

In the derivations above, (a) follows from Eq. (48) and (49), and (b) from $\tau_{b,1}, \dots, \tau_{b,K} \in [t_{n+3} - \frac{L}{2}, t_{n+1}]$ and the fact that Eq. (50) holds within this interval. We can then uniquely retrieve the $2K$ input parameters of the b^{th} burst from the $2K$ signal moments s_{m_i} of all channels, using Prony's method.

Finally, we make the observation that the inequalities in Eq. (32) and Eq. (33) impose additional constraints on the maximum separation between the Diracs in a burst b , namely on $\tau_{b,K} - \tau_{b,1}$. Specifically, we need to impose:

$$5 \int_{\tau_{b,1}}^{\tau_{b,K}} f(\tau) d\tau < \int_{\tau_{b,1}}^{\tau_{b,1} + \frac{L}{2}} f(\tau) d\tau,$$

which may give different constraints on the Dirac separation according to the filter characteristics, A_{max} and A_{min} .

REFERENCES

- [1] M. Unser. Sampling-50 years after Shannon. *Proceedings of the IEEE*, 88(4):569–587, Apr 2000.
- [2] C. E. Shannon. Communication in the presence of noise. *Proceedings of the IRE*, 37(1):10–21, Jan 1949.
- [3] E. J. Candès, J. Romberg, and T. Tao. Robust uncertainty principles: exact signal reconstruction from highly incomplete frequency information. *IEEE Transactions on Information Theory*, 52(2):489–509, Feb 2006.
- [4] D. L. Donoho. Compressed sensing. *IEEE Transactions on Information Theory*, 52(4):1289–1306, Apr 2006.
- [5] E. J. Candès and C. Fernandez-Granda. Towards a mathematical theory of super-resolution. *CoRR*, abs/1203.5871, 2012.
- [6] P. L. Dragotti, M. Vetterli, and T. Blu. Sampling Moments and Reconstructing Signals of Finite Rate of Innovation: Shannon Meets Strang-Fix. *IEEE Transactions on Signal Processing*, 55(5):1741–1757, May 2007.
- [7] M. Vetterli, P. Marziliano, and T. Blu. Sampling signals with finite rate of innovation. *IEEE Transactions on Signal Processing*, 50(6):1417–1428, Jun 2002.
- [8] R. Tur, Y. C. Eldar, and Z. Friedman. Innovation Rate Sampling of Pulse Streams With Application to Ultrasound Imaging. *IEEE Transactions on Signal Processing*, 59(4):1827–1842, Apr 2011.
- [9] Y. M. Lu and M. N. Do. A Theory for Sampling Signals from a Union of Subspaces. *IEEE Transactions on Signal Processing*, 56(6):2334–2345, Jun 2008.
- [10] C. S. Seelamantula and M. Unser. A generalized sampling method for finite-rate-of-innovation-signal reconstruction. *IEEE Signal Processing Letters*, 15:813–816, 2008.
- [11] R. Alexandru and P. L. Dragotti. Time-based Sampling and Reconstruction of Non-bandlimited Signals. *IEEE International Conference on Acoustics, Speech and Signal Processing (ICASSP'19)*, May 2019.
- [12] R. Alexandru and P. L. Dragotti. Time encoding and perfect recovery of non-bandlimited signals with an integrate-and-fire system. *IEEE International Conference on Sampling Theory and Applications (SampTA'19)*, Jul 2019.
- [13] B. F. Logan. Information in the zero crossings of bandpass signals. *The Bell System Technical Journal*, 56(4):487–510, Apr 1977.
- [14] R. Steele. *Delta Modulation Systems*. Pentech Press & Halsted Press, 1975. This book has been translated into Russian Address: London & New York.

- [15] A. A. Lazar and L. T. Toth. Perfect recovery and sensitivity analysis of time encoded bandlimited signals. *IEEE Transactions on Circuits and Systems I: Regular Papers*, 51(10):2060–2073, Oct 2004.
- [16] E.D.A. Adrian. *The basis of sensation: the action of the sense organs*. Hafner, 1928.
- [17] P. Dayan and L. F. Abbott. *Theoretical Neuroscience: Computational and Mathematical Modeling of Neural Systems*. The MIT Press, 2005.
- [18] W. Gerstner and W. Kistler. *Spiking Neuron Models: An Introduction*. Cambridge University Press, New York, NY, USA, 2002.
- [19] T. Delbrück, B. Linares-Barranco, E. Culurciello, and C. Posch. Activity-driven, event-based vision sensors. In *Proceedings of 2010 IEEE International Symposium on Circuits and Systems*, pages 2426–2429, May 2010.
- [20] A. A. Lazar. Time encoding with an integrate-and-fire neuron with a refractory period. *Neurocomputing*, 65:65–66, 2005.
- [21] A. A. Lazar and L. T. Toth. Time encoding and perfect recovery of bandlimited signals. In *2003 IEEE International Conference on Acoustics, Speech, and Signal Processing, 2003. Proceedings. (ICASSP '03)*, volume 6, pages VI–709, Apr 2003.
- [22] A. A. Lazar and E. A. Pnevmatikakis. Video Time Encoding Machines. *IEEE Transactions on Neural Networks*, 22(3):461–473, Mar 2011.
- [23] H. Feichtinger, J. Príncipe, J. Romero, A. Singh Alvarado, and G. Velasco. Approximate reconstruction of bandlimited functions for the integrate and fire sampler. *Adv. Comput. Math.*, 36(1):67–78, Jan 2012.
- [24] A. A. Lazar, E. K. Simonyi, and L. T. Toth. Fast recovery algorithms for time encoded bandlimited signals. In *Proceedings. (ICASSP '05). IEEE International Conference on Acoustics, Speech, and Signal Processing, 2005.*, volume 4, pages iv/237–iv/240 Vol. 4, Mar 2005.
- [25] K. Adam, A. Scholefield, and M. Vetterli. Multi-channel time encoding for improved reconstruction of bandlimited signals. In *2019 IEEE International Conference on Acoustics, Speech, and Signal Processing. Proceedings. (ICASSP '19)*, May 2019.
- [26] D. Florescu and D. Coca. A novel reconstruction framework for time-encoded signals with integrate-and-fire neurons. *Neural Computation*, 27(9):1872–1898, 2015.
- [27] M. Unser and A. Aldroubi. A general sampling theory for non-ideal acquisition devices. *IEEE Transactions on Signal Processing*, 42(11):2915–2925, Nov 1994.
- [28] A. Aldroubi and K. Gröchenig. Nonuniform Sampling and Reconstruction in Shift-Invariant Spaces. *SIAM Review*, 43(4):585–620, 2001.
- [29] H. Feichtinger and K. Gröchenig. Theory and practice of irregular sampling. *Wavelets: Mathematics and Applications*, Jan 1994.
- [30] D. Gontier and M. Vetterli. Sampling based on timing: Time encoding machines on shift-invariant subspaces. *Applied and Computational Harmonic Analysis*, 36(1):63 – 78, 2014.
- [31] A. A. Lazar and E. A. Pnevmatikakis. Reconstruction of sensory stimuli encoded with integrate-and-fire neurons with random thresholds. *EURASIP Journal on Advances in Signal Processing*, 2009, 2009.
- [32] R. Prony. Essai expérimental et analytique sur les lois de la dilatabilité de fluides lastiques et sur celles de la force expansive de la vapeur de leau et de la vapeur de lalkool, à différentes températures. *Journal de l'École Polytechnique*, 1(22):24–76.
- [33] M. Unser. Splines: a perfect fit for signal and image processing. *IEEE Signal Processing Magazine*, 16(6):22–38, Nov 1999.
- [34] M. Unser and T. Blu. Cardinal exponential splines: part I - theory and filtering algorithms. *IEEE Transactions on Signal Processing*, 53(4):1425–1438, Apr 2005.
- [35] G. Strang and G. Fix. *A Fourier Analysis of the Finite Element Variational Method*, pages 793–840. Springer Berlin Heidelberg, Berlin, Heidelberg, 2011.
- [36] S. B. Russ. A translation of Bolzano's paper on the intermediate value theorem. *Historia Mathematica - HIST MATH*, 7:156–185, 05 1980.
- [37] P. Stoica and R. Moses. *Spectral Analysis of Signals*. 2005.
- [38] J. A. Urigüen, T. Blu, and P. L. Dragotti. FRI Sampling With Arbitrary Kernels. *IEEE Transactions on Signal Processing*, 61(21):5310–5323, Nov 2013.
- [39] T. Blu, P. Dragotti, M. Vetterli, P. Marziliano, and L. Coulot. Sparse sampling of signal innovations. *IEEE Signal Processing Magazine*, 25(2):31–40, Mar 2008.
- [40] J. A. Cadzow. Signal enhancement-a composite property mapping algorithm. *IEEE Transactions on Acoustics, Speech, and Signal Processing*, 36(1):49–62, Jan 1988.